Goal-Oriented Adaptive Finite Element Methods for Elliptic Problems Revisited

Markus Bürg[†]and Murtazo Nazarov[‡]

April 21, 2015

Abstract

A goal-oriented a posteriori error estimation of an output functional for elliptic problems is presented. Continuous finite element approximations are used in quadrilateral and triangular meshes. The algorithm is similar to the classical dual-weighted error estimation, however the dual weight contains solutions of the proposed patch problems. The patch problems are introduced to apply Clément and Scott-Zhang type interpolation operators to estimate point values with the finite element polynomials. The algorithm is shown to be reliable, efficient and convergent.

Keywords: Poisson equation, adaptive finite element method, goal oriented error estimation, *hp*-mesh refinement, convergence of adaptive algorithm
AMS subject classifications: 65M60

1 Introduction

In this paper we develop *a goal-oriented a posteriori* error estimation with respect to certain target functionals. A goal oriented adaptive finite element method has been an active research of many scientists since last three decades and goes back to earlier work of Erikson and Johnson, Becker and Rannacher, with co-workers, see [12, 18, 4, 13, 26]. The error in the target functional, or the so-called *quantity of interest* is written as a product of the residual of the underlying primal problem and the corresponding *adjoint* or *dual solution*. Although dual-weighted *a posteriori* error estimates are applied successfully for various problems and impressive performance was obtained in terms of efficiency and compatibility, see e.g. [17, 24, 25], the convergence of the adaptive algorithm was not known until the work of [23, 22]. In [23] the dual-weighted term is kept element-wise, and by making rather stronger regularity assumptions for the primal and dual solutions they proved the convergence and optimality of the adaptive algorithm. Whereas in [22] product of the energy norms of primal and dual problems is kept globally. The estimator marks cells with respect to the energy norms of primal and dual problems separately, then the set of marked cells with the smallest cardinality is refined. The convergence and optimality of the algorithm are established for the scaled Poisson equation, however the generalization for more complex differential equations is not clear. In [16] the product of energy norms of the primal and dual problems is separated by Hölder's inequality, then the union of the sets with the largest error with respect to both primal and dual error indicators is chosen for the refinement. The approximated error is overestimated in this case, nevertheless the convergence of the underlying adaptive algorithm is obtained using the contraction framework by [8].

[‡]Division of Scientific Computing, Department of Information Technology, Uppsala University, Box 337, SE-751 05 Uppsala Sweden
[†]Department of Mathematics, Texas A&M University, Texas, USA

The presented method in this paper is closely related to the classical dual-weighted algorithm, i.e. the error on the quantity of interest is estimated by the sum of the cell errors, which are the product of the primal and dual contributions. Moreover, finite element spaces for the primal and dual solutions can be the same. The main idea consists of using Clément or Scott-Zhang type interpolation operator to estimate the continuous dual solution by a local average of the underlying finite element space. First, we prove reliability and efficiency of the new algorithm. We then prove the convergence and show the optimality of the algorithm numerically. The proof of optimality of the algorithm is under investigations and will be reported in due time.
To avoid confusion in notations between triangular and quadrilateral elements, we develop the main framework and proofs for quadrilateral meshes. Nevertheless, the below analysis also apply to triangular meshes.
The paper is organized as follows. In Section 2 we give the standard finite element notations and the problem formulation. Section 3 is the main contribution of this paper. We introduce an adaptive algorithm based on goal-oriented a posteriori error estimation, we prove its reliability, efficiency. Then in Section 3 we discuss convergence of the proposed adaptive algorithm for h and hp refinements. Number of numerical illustrations is given in Section 5 to support the theory presented in this paper.

2 Preliminaries

In this section, we want to fix some notations and introduce the basic assumptions which we require throughout this work. Further, the elliptic model problem is presented and we introduce the basic idea of goal-oriented adaptivity.

2.1 Notations and Basic Assumptions

Let $\Omega \subset \mathbb{R}^2$ denote some open and bounded domain. We denote the Lebesgue space of square-integrable functions in Ω by $L^2(\Omega)$ and its dual by $L^2(\Omega)'$. The Sobolev space $H^1(\Omega)$ is defined by

$$H^1(\Omega) := \left\{ u \in L^2(\Omega) : \nabla u \in L^2(\Omega)^2 \right\}.$$

The space $H_0^1(\Omega)$ contains all functions from $H^1(\Omega)$ with vanishing trace on the boundary $\partial\Omega$ of Ω. Let $\mathcal{T}$ be a triangulation of Ω consisting of quadrilaterals with possibly one-irregular hanging nodes. We assume that, for every $K \in \mathcal{T}$, there exists a reference mapping $F : \widehat{K} \to K$. Let $h := (h_K)_{K \in \mathcal{T}}$, $h_K := \operatorname{diam}(K)$ denote the mesh size vector and $p := (p_K)_{K \in \mathcal{T}}$, $p_K \in \mathbb{N}$ be the polynomial degree vector associated with triangulation $\mathcal{T}$. Further, we assume that $\mathcal{T}$ is (γ_h, γ_p)-regular [5, 29, 31]:

Definition 1 ((γ_h, γ_p)-Regularity)**.** *$\mathcal{T}$ is called* (γ_h, γ_p)-regular*, if and only if there exist constants $\gamma_h, \gamma_p > 0$ such that*

$$\frac{h_{K_1}}{\gamma_h} \le h_{K_2} \le \gamma_h h_{K_1}$$

and

$$\frac{p_{K_1}}{\gamma_p} \le p_{K_2} \le \gamma_p p_{K_1}$$

for all $K_1, K_2 \in \mathcal{T}$ with $K_1 \cap K_2 \neq \emptyset$.

The finite-dimensional approximation space $V^p(\mathcal{T})$ is defined by

$$V^p(\mathcal{T}) := \left\{ u \in H_0^1(\Omega) : u|_K \circ F_K \in Q_{p_K}\left(\widehat{K}\right) \text{ for all } K \in \mathcal{T} \right\},$$

where $Q_q\left(\widehat{K}\right)$ denotes the tensor-product polynomial space of degree $q \in \mathbb{N}$. An interior edge is the (nontrivial) intersection $e = K_1 \cap K_2$ of two elements $K_1, K_2 \in \mathcal{T}$ and we denote the collection of all interior edges by $\mathcal{E}(\mathcal{T})$.

Now, let $K \in \mathcal{T}$ be arbitrary. Then, we denote the set of all interior edges of cell K by $\mathcal{E}(\mathcal{T}; K)$. For $e \in \mathcal{E}(\mathcal{T}; K)$, we set $h_e := \operatorname{diam}(e)$ and $p_e := \max\{p_K, p_{K_*}\}$, where $K_* \in \mathcal{T}$ with $K \cap K_* = e$. Further, we define the patch ω_K around cell K by

$$\omega_K := \bigcup_{L \in \mathcal{T}} \{L : K \text{ and } L \text{ share a common edge}\}.$$

A slightly larger patch $\omega_{K,1}$ is defined by

$$\omega_{K,1} := \bigcup_{\substack{L \in \mathcal{T} \\ K \cap L \neq \emptyset}} L$$

and we can extend this definition iteratively by

$$\omega_{K,i+1} := \bigcup_{\substack{L \in \mathcal{T} \\ \omega_{K,i} \cap L \neq \emptyset}} L \tag{1}$$

for all $i \in \mathbb{N}$.

2.2 The Elliptic Model Problem

In this section, we want to present the elliptic model problem, which we consider throughout this work, and introduce its weak and discrete formulations. Further, the corresponding dual problems are derived. The Poisson problem with homogeneous Dirichlet boundary conditions reads as follows: Find $u : \overline{\Omega} \to \mathbb{R}$ such that

$$\begin{aligned} -\Delta u &= f \qquad \text{in } \Omega, \\ u &= 0 \qquad \text{on } \partial\Omega, \end{aligned} \tag{2}$$

where $f : \Omega \to \mathbb{R}$ denotes some right-hand side function. By multiplying the first equation with some test function $\phi \in H_0^1(\Omega)$ and performing integration by parts, we obtain the weak formulation to find $u \in H_0^1(\Omega)$ such that

$$\int_\Omega (\nabla \phi)^T \nabla u = \int_\Omega \phi f \qquad \forall \phi \in H_0^1(\Omega) \tag{3}$$

for $f \in L^2(\Omega)$. Then, its discrete formulation reads to find $u_{\mathrm{FE}} \in V^p(\mathcal{T})$ such that

$$\int_\Omega (\nabla \phi)^T \nabla u_{\mathrm{FE}} = \int_\Omega \phi f \qquad \forall \phi \in V^p(\mathcal{T}). \tag{4}$$

The basic idea of goal-oriented a posteriori error estimation is to adapt the finite-dimensional approximation space with respect to some quantity of interest $J \in L^2(\Omega)'$. From the Riesz representation theorem, it follows that there exists some $j \in L^2(\Omega)$ such that

$$J(\phi) = \int_\Omega j\phi \qquad \forall \phi \in L^2(\Omega).$$

To obtain some information about the accuracy of the finite element solution of primal problem (4) in this quantity of interest, one can solve a dual problem involving functional J. The dual problem corresponding to primal problem (3) reads to find $z \in H_0^1(\Omega)$ such that

$$\int_\Omega (\nabla z)^T \nabla \phi = J(\phi) \qquad \forall \phi \in H_0^1(\Omega) \tag{5}$$

and its discrete formulation is given by looking for $z_{\mathrm{FE}} \in V^p(\mathcal{T})$ such that

$$\int_\Omega (\nabla z_{\mathrm{FE}})^T \nabla \phi = J(\phi) \qquad \forall \phi \in V^p(\mathcal{T}). \tag{6}$$

3 Goal-Oriented Adaptivity

In this section, we want to present the idea of goal-oriented adaptivity that we rely on. The a posteriori error estimation, which we employ, is a dual-weighted residual method that is based on the product of local error indicators for the primal and dual problem. The presented method is a combination of the ideas proposed in [2, 3, 27] and [22]. Further, we propose a fully automatic *hp*-adaptive refinement strategy which is a variation of the strategy proposed in [7] for *hp*-adaptivity driven by the energy norm for the Poisson problem.

Before we are going into the details of goal-oriented a posteriori error estimation and *hp*-adaptivity, let us introduce some interpolation results which we will require later on. In [30], an H^1-conforming interpolation operator that preserves piecewise polynomial boundary conditions was introduced for the *h*-adaptive finite element method. This interpolation operator was extended to the *hp*-adaptive case in [20].

Theorem 1 (Scott-Zhang Interpolation)**.** *There exists some bounded linear operator* $\Pi^1 : H_0^1(\Omega) \to V^p(\mathcal{T})$ *and some constant* $C_{SZ} > 0$ *independent of mesh size vector* h *and polynomial degree vector* p *such that*

$$\left\|u - \Pi^1 u\right\|_{L^2(K)} + \sqrt{\frac{h_K}{p_K}} \left\|u - \Pi^1 u\right\|_{L^2(\partial K)} \leq C_{SZ} \frac{h_K}{p_K} \|\nabla u\|_{L^2(\omega_{K,1})}$$

for all $K \in \mathcal{T}$*.*

Proof. See Theorem 3.3 in [20]. □

Further, let $\Pi : L^2 \to V^p$ be an L^2 projection operator.

3.1 Energy Norm A Posteriori Error Estimation

First, let us review some results about a posteriori error estimation in the energy norm. Our goal-oriented a posteriori error estimator will be based on the residual-based a posteriori error estimator presented in this section.

The residual-based a posteriori error estimator for the *hp*-adaptive finite element method for the Poisson problem (2) was first introduced in [21]. The estimated error η is a sum of local error indicators η_K, $K \in \mathcal{T}$. These local indicators can be decomposed into a residual-based term and a jump-based term.

Definition 2 (Energy Norm A Posteriori Error Estimator (Primal Problem))**.** *Let* $u_{FE} \in V^p(\mathcal{T})$ *be the solution of (4). Then, the* residual-based a posteriori error estimator η *is defined by*

$$\eta\left(u_{FE}, \Pi f\right)^2 := \sum_{K \in \mathcal{T}} \eta_K \left(u_{FE}, \Pi f\right)^2,$$

where the local error indicators η_K can be decomposed into

$$\eta_K\left(u_{FE}, \Pi f\right)^2 := \eta_{R,K}\left(u_{FE}, \Pi f\right)^2 + \eta_{J,K}\left(u_{FE}\right)^2$$

for all $K \in \mathcal{T}$. Here, the residual-based term $\eta_{R,K}$ is given by

$$\eta_{R,K}\left(u_{FE}, \Pi f\right) := \frac{h_K}{p_K} \left\|\Pi f + \Delta u_{FE}\right\|_{L^2(K)}$$

and the jump-based term $\eta_{J,K}$ by

$$\eta_{J,K}\left(u_{FE}\right)^2 := \frac{1}{2} \sum_{e \in \mathcal{E}(\mathcal{T};K)} \frac{h_e}{p_e} \left\| \left[\frac{du_{FE}}{dn_K} \right] \right\|_{L^2(e)}^2,$$

where n_K denotes the outward-pointing unit normal vector of cell K and $[\cdot]$ the jump over edge e.

Note, this a posteriori error estimator can also be used for the dual problem (5).
The following reliability and efficiency estimates for this residual-based a posteriori error estimator have been proven in [21].

Theorem 2 (Energy Norm A Posteriori Error Estimates (Primal Problem))**.** *Let $u \in H_0^1(\Omega)$ be the solution of (3) and $u_{FE} \in V^p(\mathcal{T})$ be the solution of (4). Then:*

1. *There exists some constant $C_{rel} > 0$ independent of mesh size vector h and polynomial degree vector p such that*

$$\left\|\nabla\left(u - u_{FE}\right)\right\|_{L^2(\Omega)}^2 \leq C_{rel} \left(\eta\left(u_{FE}, \Pi f\right)^2 + \sum_{K \in \mathcal{T}} \frac{h_K^2}{p_K^2} \left\|f - \Pi f\right\|_{L^2(K)}^2 \right).$$

2. *There exists some constant $C_{\mathit{eff}} > 0$ independent of cell diameter h_K and polynomial degree p_K such that*

$$\eta_K\left(u_{FE}, \Pi f\right)^2 \leq C_{\mathit{eff}} \left(p_K^{2(1+\varepsilon)} \left\|\nabla\left(u - u_{FE}\right)\right\|_{L^2(\omega_{K,1})}^2 + \frac{h_K^2}{p_K^{1-4\varepsilon}} \left\|f - \Pi f\right\|_{L^2(\omega_{K,1})}^2 \right)$$

   for all $K \in \mathcal{T}$ and all $\varepsilon > 0$.

Proof. Choose $\alpha = 0$ in Theorem 3.6 in [21]. □

3.2 Goal-Oriented A Posteriori Error Estimation

The basic idea of goal-oriented adaptive finite element methods is to adapt the mesh according to the functional $J \in L^2(\Omega)'$ which has been introduced in Section 2.2. Therefore, we need to know how good the finite element solution $u_{\mathrm{FE}} \in V^p(\mathcal{T})$ of the discrete primal problem (4) is with respect to this quantity of interest. To get some idea about this fact, we employ the residual-based a posteriori error estimator, which has been introduced in Definition 2 for the primal problem (3), and multiply it by some appropriate weight derived from the dual problem (5).
Before we define the goal-oriented a posteriori error estimator, let us consider some auxiliary results first. The first result is a slight generalization of Lemma 3.7 in [5].

Lemma 1. *Let $K \in \mathcal{T}$ be arbitrary. Further, let $z_{FE} \in V^p(\Omega)$ be the solution of (6) and $v_K \in H_0^1(\omega_{K,2})$ be the solution of the variational problem*

$$\int_{\omega_{K,2}} (\nabla v_K)^T \nabla\phi = \int_{\omega_{K,2}} \left(j\phi - (\nabla z_{FE})^T \nabla\phi\right) \qquad \forall\phi \in H_0^1(\omega_{K,2}). \tag{7}$$

Then, it holds

$$\sup_{\phi\in H_0^1(\omega_{K,2})} \frac{\int_{\omega_{K,2}} \left(j\phi - (\nabla z_{FE})^T \nabla\phi\right)}{\|\nabla\phi\|_{L^2(\omega_{K,2})}} = \|\nabla v_K\|_{L^2(\omega_{K,2})}.$$

Proof. Replace $V_{K,j}^p(\mathcal{K}|_{\omega_K}, \omega_K)$ by $H_0^1(\omega_{K,2})$ in Lemma 3.7 in [5]. □

Note, this result can also be formulated for primal problem (3).
By replacing $H_0^1(\omega_{K,2})$ by $V^{p+1}(\mathcal{T}|_{\omega_{K,2}})$ in variational problem (7), we obtain the discrete formulation to find $v_{K,\mathrm{FE}} \in V^{p+1}(\mathcal{T}|_{\omega_{K,2}})$ such that

$$\int_{\omega_{K,2}} (\nabla v_{K,\mathrm{FE}})^T \nabla\phi = \int_{\omega_{K,2}} \left(j\phi - (\nabla z_{\mathrm{FE}})^T \nabla\phi\right) \qquad \forall\phi \in V^{p+1}(\mathcal{T}|_{\omega_{K,2}}). \tag{8}$$

Note, we cannot simply use the restriction $V^p(\mathcal{T}|_{\omega_{K,2}})$ of the global finite element space $V^p(\mathcal{T})$ to the patch here. This would imply that the right-hand side vanishes and, thus, $v_{K,\mathrm{FE}} = 0$ in $\omega_{K,2}$ for all $K \in \mathcal{T}$.
The energy error $\|\nabla(v_K - v_{K,\mathrm{FE}})\|_{L^2(\omega_{K,2})}$ can be estimated by a residual-based a posteriori error estimator for local problem (7). However, since the right-hand side of (7) has a slightly different structure than the one in primal problem (3), we cannot simply use the a posteriori error estimator from Definition 2. The following definition provides us with a residual-based a posteriori error estimator for this case.

Definition 3 (Energy Norm A Posteriori Error Estimator (Patch))**.** *Let $K \in \mathcal{T}$ be arbitrary. Further, let $v_{K,FE} \in V^{p+1}(\mathcal{T}|_{\omega_{K,2}})$ be the solution of (8) and $z_{FE} \in V^p(\mathcal{T})$ be the solution of (6). Then, the* residual-based a posteriori error estimator $\widetilde{\eta}(K)$ *is defined by*

$$\widetilde{\eta}(K)^2 := \sum_{L\in\mathcal{T}|_{\omega_{K,2}}} \widetilde{\eta}_L(K)^2,$$

where the local error indicators $\widetilde{\eta}_L$ can be decomposed into

$$\widetilde{\eta}_L^2 := \widetilde{\eta}_{R,L}^2 + \widetilde{\eta}_{J,L}^2$$

for all $L \in \mathcal{T}|_{\omega_{K,2}}$. Here, the residual-based term $\widetilde{\eta}_{R,L}$ is given by

$$\widetilde{\eta}_{R,L}(K) := \frac{h_L}{p_L} \|\Pi j + \Delta z_{FE} + \Delta v_{K,FE}\|_{L^2(L)}$$

and the jump-based term $\widetilde{\eta}_{J,L}$ by

$$\widetilde{\eta}_{J,L}(K)^2 := \frac{1}{2} \sum_{e\in\mathcal{E}(\mathcal{T}|_{\omega_{K,2}};L)} \frac{h_e}{p_e} \left\| \left[\frac{d}{dn_L}(z_{FE} + v_{K,FE})\right] \right\|_{L^2(e)}^2.$$

Before we prove some reliability and efficiency estimates for this a posteriori error estimator, let us derive some auxiliary results which will be useful in the proof. The first result collects some polynomial smoothing estimates which have been derived in [5, 6].

Lemma 2 (Polynomial Smoothing Estimates)**.** *Let $K \in \mathcal{T}$ be arbitrary and $a, b \in \mathbb{R}$ with $b > a > -\frac{1}{2}$. Then:*

1. *Let $u \in Q_{p_K}(K)$ denote some polynomial and define the smoothing function $\phi_K : K \to \mathbb{R}_+$ by*

$$\phi_K(x) := h_K^{-1} \operatorname{dist}(x, \partial K).$$

Then, there exists some constant $C_s > 0$ independent of cell diameter h_K and polynomial degree p_K such that

$$\|\phi_K^a u\|_{L^2(K)} \leq C_s p_K^{b-a} \left\|\phi_K^b u\right\|_{L^2(K)}.$$

2. *Let $e \in \mathcal{E}(\mathcal{T}; K)$ with $e = K \cap \widetilde{K}$ for some $\widetilde{K} \in \mathcal{T}$ and $u \in Q_{p_e}(e)$ denote some polynomial. We define the smoothing function $\phi_e : e \to \mathbb{R}_+$ by*

$$\phi_e(x) := \operatorname{diam}\left(K \cup \widetilde{K}\right)^{-1} \operatorname{dist}\left(x, \partial\left(K \cup \widetilde{K}\right)\right).$$

Then, there exists some constant $C_s > 0$ independent of mesh size vector h and polynomial degree vector p such that

$$\|\phi_e^a u\|_{L^2(e)} \leq C_s p_e^{b-a} \left\|\phi_e^b u\right\|_{L^2(e)}.$$

Further, there exists some extension $v_e \in H_0^1\left(K \cup \widetilde{K}\right)$ of $\phi_e^a u$ such that:

   (a) $v_e = \phi_e^a u$ on e.

   (b) There exists some constant $C_{s,tr} > 0$ independent of mesh size vector h and polynomial degree vector p such that

$$\|v_e\|_{L^2\left(K \cup \widetilde{K}\right)} \leq C_{s,tr} \frac{\sqrt{h_e}}{p_e} \|\phi_e^a u\|_{L^2(e)}.$$

   (c) There exists some constant $C_{s,inv} > 0$ independent of mesh size vector h and polynomial degree vector p such that

$$\|\nabla v_e\|_{L^2\left(K \cup \widetilde{K}\right)} \leq C_{s,inv} \frac{p_e \sqrt{p_e^{-2a} + 1}}{\sqrt{h_e}} \|\phi_e^a u\|_{L^2(e)}.$$

Proof. See Lemma 4.3 in [5]. □

The next result provides an upper bound for the residual-based term $\widetilde{\eta}_{R,L}$ of the a posteriori error estimator from Definition 3.

Lemma 3. *Let $z_{FE} \in V^p(\mathcal{T})$ be the solution of (6) and $K \in \mathcal{T}$ and $L \in \mathcal{T}|_{\omega_{K,2}}$ be arbitrary. Further, let $v_K \in H_0^1(\omega_{K,2})$ be the solution of (7) and $v_{K,FE} \in V^{p+1}\left(\mathcal{T}|_{\omega_{K,2}}\right)$ be the solution of (8). Then, there exists some constant $C > 0$ independent of cell diameter h_L and polynomial degree p_L such that*

$$\widetilde{\eta}_{R,L}(K) \leq C p_L^{\frac{3-\varepsilon}{4}} \left(\|\nabla(v_K - v_{K,FE})\|_{L^2(L)} + \frac{h_L}{p_L} \|j - \Pi j\|_{L^2(L)}\right)$$

for all $\varepsilon \in (0, 3)$.

Proof. We set $\operatorname{res} := \Pi j + \Delta z_{\mathrm{FE}} + \Delta v_{K,\mathrm{FE}}$. From Lemma 2, it follows

$$\|\operatorname{res}\|_{L^2(L)} \le C_s p_L^{\frac{1+\varepsilon}{4}} \left\| \phi_L^{\frac{1+\varepsilon}{4}} \operatorname{res} \right\|_{L^2(L)} \tag{9}$$

for all $\varepsilon > 0$. Then, we define the function $w_L : \omega_{K,2} \to \mathbb{R}$ by

$$w_L := \begin{cases} \phi_L^{\frac{1+\varepsilon}{2}} \operatorname{res}, & \text{in } L \\ 0, & \text{otherwise} \end{cases}.$$

Since $0 \le \phi_L \le \frac{1}{2}$ and $\|\nabla \phi_L\|_{L^2(L)} \le \frac{C}{h_L}$ for some constant $C > 0$ independent of h_L, it follows immediately $w_L \in H_0^1(L)$ with a standard polynomial inverse estimate (see, e.g., Theorem 4.76 in [29]). With integration by parts, we obtain

$$\begin{aligned} \left\| \phi_L^{\frac{1+\varepsilon}{4}} \operatorname{res} \right\|_{L^2(L)}^2 &= \int_L \operatorname{res} w_L \\ &= \int_L \left(j w_L - \left(\nabla\left(z_{\mathrm{FE}} + v_{K,\mathrm{FE}}\right)\right)^T \nabla w_L \right) + \int_L (j - \Pi j) w_L \\ &= \int_L \left(\nabla\left(v_K - v_{K,\mathrm{FE}}\right)\right)^T \nabla w_L + \int_L (j - \Pi j) w_L \end{aligned} \tag{10}$$

by variational problem (7). For the first term, applying the Cauchy-Schwarz inequality yields

$$\begin{aligned} \left| \int_L \left(\nabla\left(v_K - v_{K,\mathrm{FE}}\right)\right)^T \nabla w_L \right| &\le \|\nabla\left(v_K - v_{K,\mathrm{FE}}\right)\|_{L^2(L)} \|\nabla w_L\|_{L^2(L)} \\ &\le C_1 \frac{p_L^{\frac{3-\varepsilon}{2}}}{h_L} \|\nabla\left(v_K - v_{K,\mathrm{FE}}\right)\|_{L^2(L)} \left\| \phi_L^{\frac{1+\varepsilon}{4}} \operatorname{res} \right\|_{L^2(L)} \end{aligned} \tag{11}$$

for all $\varepsilon \in (0, 3)$ in exactly the same way as in the proof of Lemma 3.4 in [21]. Here, $C_1 > 0$ denotes some constant which is independent of cell diameter h_L and polynomial degree p_L. For the second term in (10), we use the L^2-property of Πj to get

$$\int_L (j - \Pi j) w_L = \int_L (j - \Pi j)\left(w_L - \Pi^1 w_L\right),$$

where $\Pi^1 : H_0^1\left(\omega_{K,2}\right) \to V^p\left(\mathcal{T}|_{\omega_{K,2}}\right)$ is the Scott-Zhang interpolation operator from Theorem 1. With the Cauchy-Schwarz inequality, this implies

$$\begin{aligned} \left| \int_L (j - \Pi j) w_L \right| &\le \|j - \Pi j\|_{L^2(L)} \left\|w_L - \Pi^1 w_L\right\|_{L^2(L)} \\ &\le C_{\mathrm{SZ}} \frac{h_L}{p_L} \|j - \Pi j\|_{L^2(L)} \|\nabla w_L\|_{L^2(L)} \end{aligned}$$

by Theorem 1, since $\operatorname{supp}(w_L) = L$. In exactly the same way as in the proof of Lemma 3.4 in [21], it follows

$$\left| \int_L (j - \Pi j) w_L \right| \le C_2 p_L^{\frac{1-\varepsilon}{2}} \|j - \Pi j\|_{L^2(L)} \left\| \phi_L^{\frac{1+\varepsilon}{4}} \operatorname{res} \right\|_{L^2(L)}, \tag{12}$$

where $C_2 > 0$ denotes some constant independent of cell diameter h_L and polynomial degree p_L. Then, inserting estimates (11) and (12) into (10) yields

$$\left\| \phi_L^{\frac{1+\varepsilon}{4}} \operatorname{res} \right\|_{L^2(L)} \le C p_L^{\frac{1-\varepsilon}{2}} \left(\frac{p_L}{h_L} \|\nabla\left(v_K - v_{K,\mathrm{FE}}\right)\|_{L^2(L)} + \|j - \Pi j\|_{L^2(L)} \right),$$

where $C := \max\{C_1, C_2\}$. Inserting into estimate (9) completes the proof. □

Next, let us consider the jump-based term $\widetilde{\eta}_{J,L}$ of the a posteriori error estimator from Definition 3.

Lemma 4. *Let $z \in H_0^1(\Omega)$ be the solution of (5) and $z_{FE} \in V^p(\mathcal{T})$ be the solution of (6). Further, let $K \in \mathcal{T}$ and $L \in \mathcal{T}|_{\omega_{K,2}}$ be arbitrary. Let $v_K \in H_0^1(\omega_{K,2})$ be the solution of (7) and $v_{K,FE} \in V^{p+1}\left(\mathcal{T}|_{\omega_{K,2}}\right)$ be the solution of (8). Then, there exists some constant $C > 0$ independent of mesh size vector h and polynomial degree vector p such that*

$$\widetilde{\eta}_{J,L}(K)^2 \leq C\left(p_L^{\frac{3+\varepsilon}{2}}\left\|\nabla\left(v_K - v_{K,FE}\right)\right\|_{L^2(\omega_{L,1})}^2 + \frac{h_L^2}{p_L^{\frac{5-\varepsilon}{2}}}\|j - \Pi j\|_{L^2(\omega_{L,1})}^2\right)$$

for all $\varepsilon \in (0,3)$.

Proof. We set

$$J := \left[\frac{d}{dn_L}\left(z_{\mathrm{FE}} + v_{K,\mathrm{FE}}\right)\right].$$

From Lemma 2, we know

$$\sum_{e \in \mathcal{E}\left(\mathcal{T}|_{\omega_{K,2}};L\right)} \frac{h_e}{p_e}\|J\|_{L^2(e)}^2 \leq C_s \sum_{e \in \mathcal{E}\left(\mathcal{T}|_{\omega_{K,2}};L\right)} \frac{h_e}{p_e^{\frac{1-\varepsilon}{2}}}\left\|\phi_e^{\frac{1+\varepsilon}{4}} J\right\|_{L^2(e)}^2 \tag{13}$$

for all $\varepsilon > 0$. Now, let $e \in \mathcal{E}\left(\mathcal{T}|_{\omega_{K,2}};L\right)$ be arbitrary. Then, there exists some cell $\widetilde{L} \in \mathcal{T}|_{\omega_{K,2}}$ such that $e = L \cap \widetilde{L}$ and some $v_e \in H_0^1(\omega_{K,2})$ such that $v_e = \phi_e^{\frac{1+\varepsilon}{2}} J$ on e by Lemma 2. Further, we define the function $\widetilde{v}_e : \omega_{K,2} \to \mathbb{R}$ by

$$\widetilde{v}_e := \begin{cases} v_e, & \text{in } L \cup \widetilde{L} \\ 0, & \text{otherwise} \end{cases}.$$

Then, we observe

$$\begin{aligned}\left\|\phi_e^{\frac{1+\varepsilon}{4}} J\right\|_{L^2(e)}^2 &= \int_e \left(\nabla\left(z_{\mathrm{FE}} + v_{K,\mathrm{FE}}\right)|_L - \nabla\left(z_{\mathrm{FE}} + v_{K,\mathrm{FE}}\right)|_{\widetilde{L}}\right)^T n_L v_e \\ &= \int_{L\cup\widetilde{L}} \left(\Delta z_{\mathrm{FE}} + \Delta v_{K,\mathrm{FE}}\right)\widetilde{v}_e + \int_{L\cup\widetilde{L}} \left(\nabla z_{\mathrm{FE}} + \nabla v_{K,\mathrm{FE}}\right)^T \nabla\widetilde{v}_e\end{aligned}$$

with the integration by parts formula. Since $v_K \in H_0^1(\omega_{K,2})$ solves (7), this reads

$$\left\|\phi_e^{\frac{1+\varepsilon}{4}} J\right\|_{L^2(e)}^2 = \int_{L\cup\widetilde{L}} \left(\Pi j + \Delta z_{\mathrm{FE}} + \Delta v_{K,\mathrm{FE}}\right)\widetilde{v}_e - \int_{L\cup\widetilde{L}} \left(\nabla\left(v_K - v_{K,\mathrm{FE}}\right)\right)^T \nabla\widetilde{v}_e + \int_{L\cup\widetilde{L}} (j - \Pi j)\widetilde{v}_e. \tag{14}$$

For the first term, using the Cauchy-Schwarz inequality gives

$$\begin{aligned}\left|\int_{L\cup\widetilde{L}} \left(\Pi j + \Delta z_{\mathrm{FE}} + \Delta v_{K,\mathrm{FE}}\right)\widetilde{v}_e\right| &\leq \left\|\Pi j + \Delta z_{\mathrm{FE}} + \Delta v_{K,\mathrm{FE}}\right\|_{L^2\left(L\cup\widetilde{L}\right)} \left\|\widetilde{v}_e\right\|_{L^2\left(L\cup\widetilde{L}\right)} \\ &\leq C_{s,\mathrm{tr}} \frac{\sqrt{h_e}}{p_e} \left\|\Pi j + \Delta z_{\mathrm{FE}} + \Delta v_{K,\mathrm{FE}}\right\|_{L^2\left(L\cup\widetilde{L}\right)} \left\|\phi_e^{\frac{1+\varepsilon}{4}} J\right\|_{L^2(e)}\end{aligned}$$

by Lemma 2 and the fact that

$$0 \leq \phi_e \leq \frac{1}{2}. \tag{15}$$

Then, Lemma 3 and the (γ_h, γ_p)-regularity of $\mathcal{T}$ yield

$$\left|\int_{L\cup\widetilde{L}} \left(\Pi j + \Delta z_{\mathrm{FE}} + \Delta v_{K,\mathrm{FE}}\right)\widetilde{v}_e\right| \leq C\frac{p_e^{\frac{3-\varepsilon}{4}}}{\sqrt{h_e}} \left\|\nabla\left(v_K - v_{K,\mathrm{FE}}\right)\right\|_{L^2\left(L\cup\widetilde{L}\right)} \left\|\phi_e^{\frac{1+\varepsilon}{4}} J\right\|_{L^2(e)}$$

for all $\varepsilon \in (0,3)$, where $C > 0$ denotes some constant independent of mesh size vector h and polynomial degree vector p. For the second term in identity (14), the Cauchy-Schwarz inequality implies

$$\begin{aligned}\left|\int_{L\cup\widetilde{L}} \left(\nabla\left(v_K - v_{K,\mathrm{FE}}\right)\right)^T \nabla\widetilde{v}_e\right| &\le \left\|\nabla\left(v_K - v_{K,\mathrm{FE}}\right)\right\|_{L^2\left(L\cup\widetilde{L}\right)} \left\|\nabla\widetilde{v}_e\right\|_{L^2\left(L\cup\widetilde{L}\right)} \\ &\le C_{s,\mathrm{inv}} \frac{p_e}{\sqrt{h_e}} \left\|\nabla\left(v_K - v_{K,\mathrm{FE}}\right)\right\|_{L^2\left(L\cup\widetilde{L}\right)} \left\|\phi_e^{\frac{1+\varepsilon}{4}} J\right\|_{L^2(e)}\end{aligned}$$

by Lemma 2 and (15). For the third term in (14), using the Cauchy-Schwarz inequality yields

$$\begin{aligned}\left|\int_{L\cup\widetilde{L}} (j - \Pi j)\widetilde{v}_e\right| &\le \|j - \Pi j\|_{L^2\left(L\cup\widetilde{L}\right)} \|\widetilde{v}_e\|_{L^2\left(L\cup\widetilde{L}\right)} \\ &\le C_{s,\mathrm{tr}} \frac{\sqrt{h_e}}{p_e} \|j - \Pi j\|_{L^2\left(L\cup\widetilde{L}\right)} \left\|\phi_e^{\frac{1+\varepsilon}{4}} J\right\|_{L^2(e)}\end{aligned}$$

by Lemma 2 and estimate (15). Then, inserting these estimates into (14) and dividing by $\left\|\phi_e^{\frac{1+\varepsilon}{4}} J\right\|_{L^2(e)}$ yields

$$\left\|\phi_e^{\frac{1+\varepsilon}{4}} J\right\|_{L^2(e)} \le C\left(\frac{p_e}{\sqrt{h_e}} \left\|\nabla\left(v_K - v_{K,\mathrm{FE}}\right)\right\|_{L^2\left(L\cup\widetilde{L}\right)} + \frac{\sqrt{h_e}}{p_e} \|j - \Pi j\|_{L^2\left(L\cup\widetilde{L}\right)}\right),$$

where $C > 0$ denotes some constant independent of mesh size vector h and polynomial degree vector p. By inserting into estimate (13), the result follows. □

Now, we are ready to prove the reliability and efficiency estimates for the a posteriori error estimator from Definition 3.

Proposition 1 (Energy Norm A Posteriori Error Estimates (Patch))**.** *Let $z \in H_0^1(\Omega)$ be the solution of (5) and $z_{FE} \in V^p(\mathcal{T})$ be the solution of (6). Further, let $K \in \mathcal{T}$ be arbitrary. Let $v_K \in H_0^1\left(\omega_{K,2}\right)$ be the solution of (7) and $v_{K,FE} \in V^{p+1}\left(\mathcal{T}|_{\omega_{K,2}}\right)$ be the solution of (8). Then:*

1. *There exists some constant $C_{rel} > 0$ independent of mesh size vector h and polynomial degree vector p such that*

$$\left\|\nabla\left(v_K - v_{K,FE}\right)\right\|^2_{L^2(\omega_{K,2})} \le C_{rel}\left(\widetilde{\eta}(K)^2 + \sum_{L\in\mathcal{T}|_{\omega_{K,2}}} \frac{h_L^2}{p_L^2} \|j - \Pi j\|^2_{L^2(L)}\right).$$

2. *There exists some constant $C_{eff} > 0$ independent of cell diameter h_L and polynomial degree p_L such that*

$$\widetilde{\eta}_L(K)^2 \le C_{eff}\left(p_L^{\frac{3+\varepsilon}{2}} \left\|\nabla\left(v_K - v_{K,FE}\right)\right\|^2_{L^2(\omega_{L,1})} + \frac{h_L^2}{p_L^{\frac{1+\varepsilon}{2}}} \|j - \Pi j\|^2_{L^2(\omega_{L,1})}\right)$$

for all $\varepsilon \in (0,3)$ and all $L \in \mathcal{T}|_{\omega_{K,2}}$.

Proof. 1. We set $e := v_K - v_{K,\mathrm{FE}}$. From the Galerkin orthogonality

$$\int_{\omega_{K,2}} (\nabla e)^T \nabla \Pi^1 e = 0,$$

we get

$$\|\nabla e\|^2_{L^2(\omega_{K,2})} = \int_{\omega_{K,2}} (\nabla e)^T \nabla\left(e - \Pi^1 e\right),$$

where $\Pi^1 : H_0^1(\omega_{K,2}) \to V^{p+1}\left(\mathcal{T}|_{\omega_{K,2}}\right)$ is the interpolation operator from Theorem 1. By using variational problem (7), it follows

$$
\begin{aligned}
\|\nabla e\|^2_{L^2(\omega_{K,2})} &= \sum_{L \in \mathcal{T}|_{\omega_{K,2}}} \int_L \Big(j\left(e - \Pi^1 e\right) - \left(\nabla\left(z_{\mathrm{FE}} + v_{K,\mathrm{FE}}\right)\right)^T \nabla\left(e - \Pi^1 e\right)\Big) \\
&= \sum_{L \in \mathcal{T}|_{\omega_{K,2}}} \Big(T_1(L) + \frac{1}{2} T_2(L) + T_3(L) \Big)
\end{aligned}
\tag{16}
$$

by integration by parts. Here, the terms T_1 and T_2 are given by

$$
\begin{aligned}
T_1(L) &:= \int_L \left(\Pi j + \Delta z_{\mathrm{FE}} + \Delta v_{K,\mathrm{FE}}\right)\left(e - \Pi^1 e\right), \\
T_2(L) &:= \sum_{f \in \mathcal{E}\left(\mathcal{T}|_{\omega_{K,2}};L\right)} \int_f \left[\frac{d v_{K,\mathrm{FE}}}{d n_L} + \frac{d z_{\mathrm{FE}}}{d n_L}\right]\left(e - \Pi^1 e\right),
\end{aligned}
$$

and

$$
T_3(L) := \int_L (j - \Pi j)\left(e - \Pi^1 e\right)
$$

for all $L \in \mathcal{T}|_{\omega_{K,2}}$. For the first term, using the Cauchy-Schwarz inequality gives

$$
\begin{aligned}
T_1(L) &\le \|\Pi j + \Delta z_{\mathrm{FE}} + \Delta v_{K,\mathrm{FE}}\|_{L^2(L)} \left\|e - \Pi^1 e\right\|_{L^2(L)} \\
&\le C_{\mathrm{SZ}} \frac{h_L}{p_L} \|\Pi j + \Delta z_{\mathrm{FE}} + \Delta v_{K,\mathrm{FE}}\|_{L^2(L)} \|\nabla e\|_{L^2(\omega_{L,1})}
\end{aligned}
$$

by Theorem 1. For the second term, we obtain

$$
\begin{aligned}
T_2(L) &\le \sum_{f \in \mathcal{E}\left(\mathcal{T}|_{\omega_{K,2}};L\right)} \left\| \left[\frac{d v_{K,\mathrm{FE}}}{d n_L} + \frac{d z_{\mathrm{FE}}}{d n_L}\right] \right\|_{L^2(f)} \left\|e - \Pi^1 e\right\|_{L^2(f)} \\
&\le C_{\mathrm{SZ}} \sum_{f \in \mathcal{E}\left(\mathcal{T}|_{\omega_{K,2}};L\right)} \sqrt{\frac{h_f}{p_f}} \left(\left\| \left[\frac{d v_{K,\mathrm{FE}}}{d n_L}\right] \right\|_{L^2(f)} + \left\| \left[\frac{d z_{\mathrm{FE}}}{d n_L}\right] \right\|_{L^2(f)} \right) \|\nabla e\|_{L^2(\omega_{L,1})}
\end{aligned}
$$

with the same arguments and the (γ_h, γ_p)-regularity of $\mathcal{T}$. For the third term T_3, we get

$$
\begin{aligned}
T_3(L) &\le \|j - \Pi j\|_{L^2(L)} \left\|e - \Pi^1 e\right\|_{L^2(L)} \\
&\le C_{\mathrm{SZ}} \frac{h_L}{p_L} \|j - \Pi j\|_{L^2(L)} \|\nabla e\|_{L^2(\omega_{L,1})}
\end{aligned}
$$

with the same arguments. Inserting these estimates into (16) and using the discrete Cauchy-Schwarz inequality implies

$$
\|\nabla e\|^2_{L^2(\omega_{K,2})} \le C \left(\widetilde{\eta}(K) + \sum_{L \in \mathcal{T}|_{\omega_{K,2}}} \frac{h_L}{p_L} \|j - \Pi j\|_{L^2(L)} \right) \|\nabla e\|_{L^2(\omega_{K,2})},
$$

where $C > 0$ denotes some constant independent of mesh size vector h and polynomial degree vector p.

2. Follows immediately from Lemmas 3 and 4.

□

Now, let us define the goal-oriented a posteriori error estimator ζ. As usual, this error estimator can be decomposed into local error indicators ζ_K. They are constructed as the product of the local indicator η_K from the energy norm a posteriori error estimator η derived for primal problem (3) and the full energy norm error estimator $\widetilde{\eta}(K)$ derived for variational problem (7) plus the energy norm $\|\nabla v_{K,\mathrm{FE}}\|_{L^2(\omega_{K,2})}$ of the solution of discrete variational problem (8). This second term serves as the local weight taking into account the relevance of cell $K \in \mathcal{T}$ to the error in the quantity of interest $|J(u) - J(u_{\mathrm{FE}})|$. This is the major difference to the results in [22] where the product of the global a posteriori error estimators for the primal and dual problem is chosen.

Definition 4 (Goal-Oriented A Posteriori Error Estimator)**.** *Let $u_{FE} \in V^p(\mathcal{T})$ be the solution of (3) and $v_{K,FE} \in V^{p+1}\left(\mathcal{T}|_{\omega_{K,2}}\right)$ be the solution of (8) for all $K \in \mathcal{T}$. Then, the* goal-oriented a posteriori error estimator ζ *is defined by*

$$\zeta := \sum_{K \in \mathcal{T}} \zeta_K,$$

where the local error indicators ζ_K are given by

$$\zeta_K := \rho_K \eta_K \left(u_{FE}, \Pi f\right)$$

for all $K \in \mathcal{T}$. Here, the local weight ρ_K is defined by

$$\rho_K := \widetilde{\eta}(K) + \|\nabla v_{K,FE}\|_{L^2(\omega_{K,2})}.$$

Before we are going to derive some reliability and efficiency estimates for this goal-oriented a posteriori error estimator, let us provide some auxiliary results which will be useful in the proof. The first result gives an upper bound for the quasi-local energy error $\|\nabla (z - z_{\mathrm{FE}})\|_{L^2(\omega_{K,1})}$ on patch $\omega_{K,1}$ in terms of the energy norm $\|\nabla v_K\|_{L^2(\omega_{K,2})}$ of the solution of variational problem (7) on a slightly larger patch $\omega_{K,2}$.

Lemma 5. *Let $z \in H_0^1(\Omega)$ be the solution of (5) and $z_{FE} \in V^p(\mathcal{T})$ be the solution of (6). Further, let $K \in \mathcal{T}$ be arbitrary and $v_K \in H_0^1(\omega_{K,2})$ be the solution of (7). Then, there exists some constant $C > 0$ independent of cell diameter h_K and polynomial degree p_K such that*

$$\|\nabla (z - z_{FE})\|_{L^2(\omega_{K,1})} \leq C \|\nabla v_K\|_{L^2(\omega_{K,2})}.$$

Proof. Let $\phi : \omega_{K,2} \to \mathbb{R}_+$ be some smoothing function such that $\phi = 1$ in $\omega_{K,1}$, $\phi \leq 1$ in $\omega_{K,2}$, and $\phi^\varepsilon (z - z_{\mathrm{FE}}) \in H_0^1(\omega_{K,2})$ for all $\varepsilon > 0$. Then, we see

(17)
$$\begin{aligned}\int_{\omega_{K,2}} (\nabla (z - z_{\mathrm{FE}}))^T \nabla (\phi^\varepsilon (z - z_{\mathrm{FE}})) &= \int_{\omega_{K,2}} \phi^\varepsilon |\nabla (z - z_{\mathrm{FE}})|^2 + \varepsilon \int_{\omega_{K,2}} \phi^{\varepsilon - 1} (z - z_{\mathrm{FE}}) (\nabla (z - z_{\mathrm{FE}}))^T \nabla \phi \\ &\geq \frac{1}{2} \|\phi^\varepsilon \nabla (z - z_{\mathrm{FE}})\|_{L^2(\omega_{K,2})}^2\end{aligned}$$

for $\varepsilon > 0$ small enough. In the same fashion, we obtain

$$\begin{aligned}\|\nabla (\phi^\varepsilon (z - z_{\mathrm{FE}}))\|_{L^2(\omega_{K,2})}^2 = \int_{\omega_{K,2}} \phi^{2\varepsilon} |\nabla (z - z_{\mathrm{FE}})|^2 &+ \varepsilon^2 \int_{\omega_{K,2}} \phi^{2(\varepsilon-1)} (z - z_{\mathrm{FE}})^2 |\nabla \phi|^2 \\ &+ 2\varepsilon \int_{\omega_{K,2}} \phi^{2\varepsilon - 1} (z - z_{\mathrm{FE}}) (\nabla (z - z_{\mathrm{FE}}))^T \nabla \phi\end{aligned}$$

and it follows

$$\|\nabla (\phi^\varepsilon (z - z_{\mathrm{FE}}))\|_{L^2(\omega_{K,2})}^2 \leq 4 \|\phi^\varepsilon \nabla (z - z_{\mathrm{FE}})\|_{L^2(\omega_{K,2})}^2 \tag{18}$$

for $\varepsilon > 0$ small enough. Then, combining estimates (17) and (18) yields

$$\frac{\int_{\omega_{K,2}} \left(\nabla\left(z - z_{\mathrm{FE}}\right)\right)^T \nabla\left(\phi^\varepsilon\left(z - z_{\mathrm{FE}}\right)\right)}{\left\|\nabla\left(\phi^\varepsilon\left(z - z_{\mathrm{FE}}\right)\right)\right\|_{L^2(\omega_{K,2})}} \geq \frac{1}{4}\left\|\phi^\varepsilon \nabla\left(z - z_{\mathrm{FE}}\right)\right\|_{L^2(\omega_{K,2})}$$
$$\geq \frac{1}{4}\left\|\nabla\left(z - z_{\mathrm{FE}}\right)\right\|_{L^2(\omega_{K,1})}$$

and we get

$$\left\|\nabla\left(z - z_{\mathrm{FE}}\right)\right\|_{L^2(\omega_{K,1})} \leq 4 \sup_{w \in H_0^1(\omega_{K,2})} \frac{\int_{\omega_{K,2}} \left(\nabla\left(z - z_{\mathrm{FE}}\right)\right)^T \nabla w}{\|\nabla w\|_{L^2(\omega_{K,2})}},$$

since $\phi^\varepsilon\left(z - z_{\mathrm{FE}}\right) \in H_0^1\left(\omega_{K,2}\right)$. Since $z \in H_0^1(\Omega)$ solves (5), we have

$$\left\|\nabla\left(z - z_{\mathrm{FE}}\right)\right\|_{L^2(\omega_{K,1})} \leq 4 \sup_{w \in H_0^1(\omega_{K,2})} \frac{\int_{\omega_{K,2}} \left(jw - \left(\nabla\left(z_{\mathrm{FE}}\right)\right)^T \nabla w\right)}{\|\nabla w\|_{L^2(\omega_{K,2})}}$$

and the result follows with Lemma 1. □

Similarly, we can also bound the sum of the energy error $\left\|\nabla\left(v_K - v_{K,\mathrm{FE}}\right)\right\|_{L^2(\omega_{K,2})}$ and the energy norm $\left\|\nabla v_{K,\mathrm{FE}}\right\|_{L^2(\omega_{K,2})}$ of the solution of patch problem (8) by the energy error $\left\|\nabla\left(z - z_{\mathrm{FE}}\right)\right\|_{L^2(\omega_{K,2})}$ of dual problem (5).

Lemma 6. *Let $z \in H_0^1(\Omega)$ be the solution of (5) and $z_{FE} \in V^p(\mathcal{T})$ be the solution of (6). Further, let $K \in \mathcal{T}$ be arbitrary. Let $v_K \in H_0^1\left(\omega_{K,2}\right)$ be the solution of (7) and $v_{K,FE} \in V^{p+1}\left(\omega_{K,2}\right)$ be the solution of (8). Then, there exists some constant $C > 0$ independent of cell diameter h_K and polynomial degree p_K such that*

$$\left\|\nabla\left(v_K - v_{K,FE}\right)\right\|_{L^2(\omega_{K,2})} + \left\|\nabla v_{K,FE}\right\|_{L^2(\omega_{K,2})} \leq C\left\|\nabla\left(z - z_{FE}\right)\right\|_{L^2(\omega_{K,2})}.$$

Proof. We see easily

$$\left\|\nabla\left(v_K - v_{K,\mathrm{FE}}\right)\right\|_{L^2(\omega_{K,2})} \leq \left\|\nabla v_K\right\|_{L^2(\omega_{K,2})} + \left\|\nabla v_{K,\mathrm{FE}}\right\|_{L^2(\omega_{K,2})}. \tag{19}$$

For the first term $\left\|\nabla v_K\right\|_{L^2(\omega_{K,2})}$, variational problem (7) yields

$$\begin{aligned}\left\|\nabla v_K\right\|^2_{L^2(\omega_{K,2})} &= \int_{\omega_{K,2}} \left(\nabla v_K\right)^T \nabla v_K \\ &= \int_{\omega_{K,2}} \left(jv_K - \left(\nabla z_{\mathrm{FE}}\right)^T \nabla v_K\right) \\ &= \int_{\omega_{K,2}} \left(\nabla\left(z - z_{\mathrm{FE}}\right)\right)^T \nabla v_K\end{aligned}$$

by dual problem (5) and, with the Cauchy-Schwarz inequality, it follows

$$\left\|\nabla v_K\right\|^2_{L^2(\omega_{K,2})} \leq \left\|\nabla\left(z - z_{\mathrm{FE}}\right)\right\|_{L^2(\omega_{K,2})} \left\|\nabla v_K\right\|_{L^2(\omega_{K,2})}. \tag{20}$$

For the second term $\left\|\nabla v_{K,\mathrm{FE}}\right\|_{L^2(\omega_{K,2})}$, variational problem (8) yields

$$\begin{aligned}\left\|\nabla v_{K,\mathrm{FE}}\right\|^2_{L^2(\omega_{K,2})} &= \int_{\omega_{K,2}} \left(\nabla v_{K,\mathrm{FE}}\right)^T \nabla v_{K,\mathrm{FE}} \\ &= \int_{\omega_{K,2}} \left(jv_{K,\mathrm{FE}} - \left(\nabla z_{\mathrm{FE}}\right)^T \nabla v_{K,\mathrm{FE}}\right) \\ &= \int_{\omega_{K,2}} \left(\nabla\left(z - z_{\mathrm{FE}}\right)\right)^T \nabla v_{K,\mathrm{FE}}\end{aligned}$$

with dual problem (5) and, by applying the Cauchy-Schwarz inequality, it follows

$$\|\nabla v_{K,\mathrm{FE}}\|^2_{L^2(\omega_{K,2})} \leq \|\nabla (z - z_{\mathrm{FE}})\|_{L^2(\omega_{K,2})} \|\nabla v_{K,\mathrm{FE}}\|_{L^2(\omega_{K,2})}. \tag{21}$$

Inserting estimates (20) and (21) into (19) completes the proof. □

Now, we are ready to prove some reliability and efficiency estimates for the goal-oriented a posteriori error estimator from Definition 4.

Theorem 3 (Goal-Oriented A Posteriori Error Estimates)**.** *Let $u \in H^1_0(\Omega)$ be the solution of (3) and $u_{FE} \in V^p(\mathcal{T})$ be the solution of (4). Further, let $z \in H^1_0(\Omega)$ be the solution of (5) and $z_{FE} \in V^p(\mathcal{T})$ be the solution of (6). Then:*

1. *There exists some constant $C_{rel} > 0$ independent of mesh size vector h and polynomial degree vector p such that*

$$|J(u) - J(u_{FE})| \leq C_{rel} \sum_{K\in\mathcal{T}} \left(\rho_K + \frac{h_K}{p_K}\|j - \Pi j\|_{L^2(\omega_{K,2})}\right)\left(\eta_K(u_{FE}, \Pi f) + \frac{h_K}{p_K}\|f - \Pi f\|_{L^2(K)}\right).$$

2. *There exists some constant $C_{\mathit{eff}} > 0$ independent of cell diameter h_K and polynomial degree p_K such that*

$$\zeta_K \leq C_{\mathit{eff}} \left(p_K^{\frac{3+\varepsilon}{4}} \|\nabla (z - z_{FE})\|_{L^2(\omega_{K,3})} + \frac{h_K}{p_K^{\frac{1+\varepsilon}{4}}}\|j - \Pi j\|_{L^2(\omega_{K,3})}\right)$$
$$\times \left(p_K^{1+\varepsilon} \|\nabla (u - u_{FE})\|_{L^2(\omega_{K,1})} + \frac{h_K}{p_K^{\frac{1}{2}-2\varepsilon}}\|f - \Pi f\|_{L^2(\omega_{K,1})}\right)$$

   for all $K \in \mathcal{T}$ and all $\varepsilon \in (0,3)$.

Proof. 1. From dual problem (5), we have

$$J(u) = \int_\Omega (\nabla z)^T \nabla u$$

as well as

$$J(u_{\mathrm{FE}}) = \int_\Omega (\nabla z)^T \nabla u_{\mathrm{FE}}.$$

We set $e := z - z_{\mathrm{FE}}$. Then, it holds

$$\begin{aligned} J(u) - J(u_{\mathrm{FE}}) &= \int_\Omega (\nabla z)^T \nabla (u - u_{\mathrm{FE}}) \\ &= \int_\Omega \left(\nabla \left(e - \Pi^1 e\right)\right)^T \nabla (u - u_{\mathrm{FE}}) \end{aligned}$$

by the Galerkin orthogonality

$$\int_\Omega \left(\nabla \left(z_{\mathrm{FE}} + \Pi^1 e\right)\right)^T \nabla (u - u_{\mathrm{FE}}) = 0,$$

where $\Pi^1 : H^1_0(\Omega) \to V^p(\mathcal{T})$ is the interpolation operator from Theorem 1. Since $u \in H^1_0(\Omega)$ solves (3), we obtain

$$\begin{aligned} J(u) - J(u_{\mathrm{FE}}) &= \sum_{K\in\mathcal{T}} \left(\int_K \left(e - \Pi^1 e\right)(f + \Delta u_{\mathrm{FE}}) + \frac{1}{2}\sum_{f\in\mathcal{E}(\mathcal{T};K)} \int_e \left(e - \Pi^1 e\right)\left[\frac{du_{\mathrm{FE}}}{dn_K}\right]\right) \\ &= \sum_{K\in\mathcal{T}} \left(T_1(K) + T_2(K) + \frac{1}{2}T_3(K)\right) \end{aligned} \tag{22}$$

with integration by parts, where the terms T_1, T_2, and T_3 are given by

$$T_1(K) := \int_K \left(e - \Pi^1 e\right) \left(\Pi f + \Delta u_{\mathrm{FE}}\right),$$
$$T_2(K) := \int_K \left(e - \Pi^1 e\right) (f - \Pi f),$$

and

$$T_3(K) := \sum_{f \in \mathcal{E}(\mathcal{T};K)} \int_e \left(e - \Pi^1 e\right) \left[\frac{du_{\mathrm{FE}}}{dn_K}\right].$$

Here, Πf denotes the local L^2-interpolation of the right-hand side function f.
Now, let $K \in \mathcal{T}$ be arbitrary. For the first term T_1, using the Cauchy-Schwarz inequality yields

$$\begin{aligned} T_1(K) &\leq \|\Pi f + \Delta u_{\mathrm{FE}}\|_{L^2(K)} \left\|e - \Pi^1 e\right\|_{L^2(K)} \\ &\leq C_{\mathrm{SZ}} \frac{h_K}{p_K} \|\Pi f + \Delta u_{\mathrm{FE}}\|_{L^2(K)} \|\nabla e\|_{L^2(\omega_{K,1})} \end{aligned}$$

by Theorem 1. With Definition 2, this reads

$$T_1(K) \leq C_{\mathrm{SZ}} \eta_{R,K} \left(u_{\mathrm{FE}}, \Pi f\right) \|\nabla e\|_{L^2(\omega_{K,1})}. \tag{23}$$

For the second term T_2, we get

$$\begin{aligned} T_2(K) &\leq \|f - \Pi f\|_{L^2(K)} \left\|e - \Pi^1 e\right\|_{L^2(K)} \\ &\leq C_{\mathrm{SZ}} \frac{h_K}{p_K} \|f - \Pi f\|_{L^2(K)} \|\nabla e\|_{L^2(\omega_{K,1})} \end{aligned} \tag{24}$$

with the same arguments. For the third term T_3, we use the Cauchy-Schwarz inequality to obtain

$$\begin{aligned} T_3(K) &\leq \sum_{f \in \mathcal{E}(\mathcal{T};K)} \left\| \left[\frac{du_{\mathrm{FE}}}{dn_K}\right] \right\|_{L^2(e)} \left\|e - \Pi^1 e\right\|_{L^2(e)} \\ &\leq C_{\mathrm{SZ}} \sum_{f \in \mathcal{E}(\mathcal{T};K)} \sqrt{\frac{h_e}{p_e}} \left\| \left[\frac{du_{\mathrm{FE}}}{dn_K}\right] \right\|_{L^2(e)} \|\nabla e\|_{L^2(\omega_{K,1})} \end{aligned}$$

by Theorem 1 and the (γ_h, γ_p)-regularity of $\mathcal{T}$. This implies

$$T_3(K) \leq 4 C_{\mathrm{SZ}} \eta_{J,K} \left(u_{\mathrm{FE}}\right) \|\nabla e\|_{L^2(\omega_{K,1})} \tag{25}$$

with Definition 2. Inserting estimates (23)-(25) into (22) implies

$$|J(u) - J\left(u_{\mathrm{FE}}\right)| \leq C \sum_{K \in \mathcal{T}} \left(\eta_{R,K} \left(u_{\mathrm{FE}}, \Pi f\right) + \eta_{J,K} \left(u_{\mathrm{FE}}\right) + \frac{h_K}{p_K} \|f - \Pi f\|_{L^2(K)}\right) \|\nabla e\|_{L^2(\omega_{K,1})},$$

where $C := \max\{C_{\mathrm{SZ}}, 2\}$. With Definition 2, it follows

$$|J(u) - J\left(u_{\mathrm{FE}}\right)| \leq C \sum_{K \in \mathcal{T}} \left(2\eta_K \left(u_{\mathrm{FE}}, \Pi f\right) + \frac{h_K}{p_K} \|f - \Pi f\|_{L^2(K)}\right) \|\nabla e\|_{L^2(\omega_{K,1})}. \tag{26}$$

Now, let $K \in \mathcal{T}$ be arbitrary. Further, let $v_K \in H_0^1\left(\omega_{K,2}\right)$ be the solution of (7) and $v_{K,\mathrm{FE}} \in V^{p+1}\left(\omega_{K,2}\right)$ be the solution of (8). Then, using Lemma 5 gives

$$\begin{aligned} \|\nabla e\|_{L^2(\omega_{K,1})} &\leq C \|\nabla v_K\|_{L^2(\omega_{K,2})} \\ &\leq C \left(\|\nabla \left(v_K - v_{K,\mathrm{FE}}\right)\|_{L^2(\omega_{K,2})} + \|\nabla v_{K,\mathrm{FE}}\|_{L^2(\omega_{K,2})}\right) \end{aligned}$$

and, after inserting into (26), the result follows with Proposition 1.

2. Let $K \in \mathcal{T}$ be arbitrary. From Definition 4, we have

$$\begin{aligned}\zeta_K &= \rho_K \eta_K \left(u_{\mathrm{FE}}, \Pi f\right) \\ &= \left(\widetilde{\eta}(K) + \left\|\nabla v_{K,\mathrm{FE}}\right\|_{L^2(\omega_{K,2})}\right) \eta_K \left(u_{\mathrm{FE}}, \Pi f\right).\end{aligned}$$

For the energy norm error estimator $\widetilde{\eta}$ for variational problem (7), it follows

$$\begin{aligned}\widetilde{\eta}(K)^2 &= \sum_{L \in \mathcal{T}|_{\omega_{K,2}}} \widetilde{\eta}_L(K)^2 \\ &\leq C_{\mathrm{eff}} \left(p_K^{\frac{3+\varepsilon}{2}} \left\|\nabla \left(v_K - v_{K,\mathrm{FE}}\right)\right\|^2_{L^2(\omega_{K,3})} + \frac{h_K^2}{p_K^{\frac{1+\varepsilon}{2}}} \left\|j - \Pi j\right\|^2_{L^2(\omega_{K,3})} \right)\end{aligned}$$

for all $\varepsilon \in (0,3)$ by Proposition 1 and the (γ_h, γ_p)-regularity of $\mathcal{T}$. Then, the result follows with Lemma 6 and Theorem 2.

□

3.3 The hp-Adaptive Refinement Strategy

In this section, we present the fully automatic hp-adaptive refinement strategy which we want to consider in this work. This strategy is based on the solution of local boundary values problems on small patches and was introduced in [7] for the Poisson problem in connection with energy norm a posteriori error estimation.

3.3.1 The Refinement Patterns

Quadrilateral mesh

We call a quasi-local, discrete enhancement of the finite element space a refinement pattern. For h-adaptive refinement, the classical refinement pattern is equally-weighted bisection in every coordinate direction. If we perform such an h-refinement step on some cell $K \in \mathcal{T}$, it may happen that we introduce some hanging nodes on the edges of K. This means that we might not obtain the full error reduction for this cell, because some degrees of freedom are constrained away. To avoid this scenario, we extend the h-refinement at least anisotropically also to the neighboring cells of K which share at least one common edge with cell K. This refinement pattern is depicted in Figure 1 on the left-hand side.

For p-adaptive refinement, the classical choice is to increase the polynomial degree p_K of cell $K \in \mathcal{T}$ by one. Also in this case, it may happen that some degrees of freedom located on the boundary of K are constrained away. To avoid this scenario, we also extend the p-refinement to the neighboring cells of K which share at least one common edge with cell K. This refinement pattern is shown in Figure 1 on the right-hand side.

Besides these two classical refinement patterns, our hp-adaptive refinement strategy is capable of supporting any other refinement pattern one can think of, e.g., anisotropic h-refinement, increase of the polynomial degree by 2, 3, …, etc. Without loss of generality, we may assume that we have $n \geq 2$ different refinement patterns to choose from.

Triangular mesh

For the triangular meshes we use the Rivara recursive bisection algorithm, see [28]. First this algorithm bisects the longest edge, then recursively repeats the bisection of the neighboring triangles of the edge

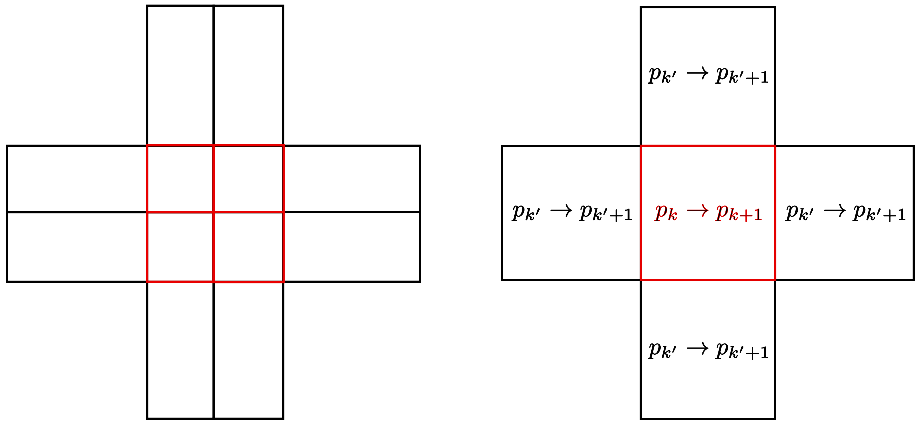

Figure 1: Refinement Patterns. Left: h-refinement. Right: p-refinement.

containing the hanging node until this edge is a common longest edge of a cell.

3.3.2 The Convergence Indicators

Let $K \in \mathcal{T}$ be arbitrary. For every $j \in \{1, \ldots, n\}$, we denote the finite element space consisting of piecewise polynomials compactly supported in ω_K with refinement pattern j applied to cell K by $V^p_{K,j}\left(\mathcal{T}|_{\omega_K}\right)$. Then, let $\kappa_{K,j} \in \mathbb{R}_+$ be the solution of the optimization problem

$$\kappa_{K,j}\zeta_K = \sup_{\phi \in V^p_{K,j}\left(\mathcal{T}|_{\omega_K}\right)} \frac{\int_{\omega_K} \left(\phi \Pi f - (\nabla\phi)^T \nabla u_{\mathrm{FE}}\right)}{\|\nabla\phi\|_{L^2(\omega_K)}}, \tag{27}$$

where $u_{\mathrm{FE}} \in V^p(\mathcal{T})$ is the solution of (4). From Lemma 1, we know that it suffices to solve the local variational problem

$$\int_{\omega_K} (\nabla\phi)^T \nabla v_{K,\mathrm{FE}} = \int_{\omega_K} \left(\phi \Pi f - (\nabla\phi)^T \nabla u_{\mathrm{FE}}\right) \qquad \forall \phi \in V^p_{K,j}\left(\mathcal{T}|_{\omega_K}\right)$$

to compute the right-hand side of (27). This way, no expensive tools from numerical optimization are necessary, but it suffices to solve a simple boundary value problem on the patch ω_K, to compute the convergence indicator $\kappa_{K,j}$.

3.3.3 Marking Cells for Refinement

For classical h-refinement, one possibility to mark cells for refinement is the fixed fraction approach presented in [10]. For energy norm a posteriori error estimation for primal problem (3), it reads to find a set $\mathcal{A} \subseteq \mathcal{T}$ such that

$$\sum_{K \in \mathcal{A}} \eta_K \left(u_{\mathrm{FE}}, \Pi f\right)^2 \geq \theta^2 \eta \left(u_{\mathrm{FE}}, \Pi f\right)^2 \tag{28}$$

for some $\theta \in (0, 1]$. Here, $u_{\mathrm{FE}} \in V^p(\mathcal{T})$ is the solution of (4). Then, convergence of the resulting h-adaptive refinement algorithm was proven in [10].

Theorem 4 (Convergence (Energy Error, h-adaptive))**.** *Let $N, r \in \mathbb{N}_0$ be arbitrary and $u \in H^1_0(\Omega)$ be the solution of (3). Further, let $\mathcal{A}_N \subseteq \mathcal{T}_N$ be such that (28) holds for some $\theta \in (0, 1]$. Let $u_N \in V^p\left(\mathcal{T}_N\right)$,* *where* $p := (r)_{K\in\mathcal{T}_N}$, *and* $u_{N+1} \in V^p(\mathcal{T}_{N+1})$, *where* $p := (r)_{K\in\mathcal{T}_{N+1}}$, *be the solutions of (4) in iteration steps* N *and* $N+1$, *respectively. Additionally, let us assume that there exists some* $\tau \in (0,1]$ *sufficiently small such that*

$$\sum_{K\in\mathcal{T}_N} h_K^2 \|f - \Pi f\|_{L^2(K)}^2 \leq \tau^2 \eta\left(u_N, \Pi f\right)^2.$$

Then, there exists some $\mu(\theta) \in (0,1)$ *independent of mesh size vector* h *such that*

$$\left\|\nabla\left(u - u_{N+1}\right)\right\|_{L^2(\Omega)} \leq \mu(\theta)\left\|\nabla\left(u - u_N\right)\right\|_{L^2(\Omega)}.$$

Proof. See Theorem 1 in [10]. □

Note, this result can also be formulated for dual problem (5).
For goal-oriented a posteriori error estimation, we can now simply replace the energy norm error estimator by the goal-oriented a posteriori error estimator from Definition 4. Thus, we mark the cells for refinement by looking for a set $\mathcal{A} \subseteq \mathcal{T}$ with minimal cardinality such that

$$\sum_{K\in\mathcal{A}} \zeta_K \geq \theta\zeta \tag{29}$$

for some $\theta \in (0,1]$.
Now, let us consider the case of *hp*-adaptive refinement. Here, we employ basically the same scheme as has been used for *h*-adaptive refinement, but modify it slightly in order to accommodate the choice between the n different refinement patterns. In Section 3.3.2, we have obtained a convergence indicator $\kappa_{K,j} \in \mathbb{R}_+$ for every cell $K \in \mathcal{T}$ and every refinement pattern $j \in \{1,\ldots,n\}$. This number tells us which refinement pattern performs best on cell K. However, this information alone might not be sufficient. We would also like to take into account the amount of work which is required to achieve the predicted error reduction. Therefore, we define so-called work-load numbers $w_{K,j} \in \mathbb{N}$ to be the dimension of the local finite element space $V_{K,j}^p(\mathcal{T}|_{\omega_K})$. Then, we mark cells for refinement by looking for a solution $\left(\mathcal{A}, (j_K)_{K\in\mathcal{A}}\right)$, $\mathcal{A} \subseteq \mathcal{T}$, of the maximization problem

$$\sum_{K\in\mathcal{A}} \frac{\kappa_{K,j_K}}{w_{K,j_K}} = \max \tag{30}$$

under the constraint

$$\sum_{K\in\mathcal{A}} \kappa_{K,j_K}^2 \eta_K\left(u_{\mathrm{FE}}, \Pi f\right)^2 \geq \theta^2 \eta\left(u_{\mathrm{FE}}, \Pi f\right)^2 \tag{31}$$

for some $\theta \in (0,1]$. Here, $u_{\mathrm{FE}} \in V^p(\mathcal{T})$ denotes the solution of (3). A convergence result for this fully automatic *hp*-adaptive refinement strategy was proven in [7, 11].

Theorem 5 (Convergence (Energy Error, *hp*-adaptive))**.** *Let* $N \in \mathbb{N}_0$ *be arbitrary and* $u \in H_0^1(\Omega)$ *be the solution of (3). Further, let* $\mathcal{A}_N \subseteq \mathcal{T}_N$ *be such that (30), (31) holds for some* $\theta \in (0,1]$. *Let* $u_N \in V^p(\mathcal{T}_N)$ *and* $u_{N+1} \in V^p(\mathcal{T}_{N+1})$ *be the solutions of (4) in iteration steps* N *and* $N+1$, *respectively. Additionally, let us assume that there exists some* $\tau \in (0,1]$ *sufficiently small such that*

$$\sum_{K\in\mathcal{T}_N} \frac{h_K^2}{p_K^2} \|f - \Pi f\|_{L^2(K)}^2 \leq \tau^2 \eta\left(u_N, \Pi f\right)^2.$$

Then, there exists some $\mu(\theta) \in (0,1)$ *independent of mesh size vector* h *and polynomial degree vector* p *such that*

$$\left\|\nabla\left(u - u_{N+1}\right)\right\|_{L^2(\Omega)} \leq \mu(\theta)\left\|\nabla\left(u - u_N\right)\right\|_{L^2(\Omega)}.$$

Proof. See Theorem 3 in [7]. □

Note, this result can also be formulated for dual problem (5).
For goal-oriented a posteriori error estimation, we can now simply replace the energy norm error estimator by the goal-oriented a posteriori error estimator from Definition 4 as we did in the h-adaptive case. Thus, we mark the cells for refinement by looking for a solution $\left(\mathcal{A},(j_K)_{K\in\mathcal{A}}\right)$, where $\mathcal{A}\subset\mathcal{T}$ with minimal cardinality, of maximization problem (30) under the constraint

$$\sum_{K\in\mathcal{A}}\kappa_{K,j_K}\zeta_K\geq\theta\zeta \tag{32}$$

for some $\theta\in(0,1]$. Unfortunately, this problem is NP-hard and, thus, cannot be solved in polynomial time [9]. Therefore, we follow the idea from [7] and use the following method to approximate a solution of maximization problem (30), (32): In a first step, we define the numbers $j_K\in\{1,\ldots,n\}$, $K\in\mathcal{T}$, by

$$j_K:=\underset{j\in\{1,\ldots,n\}}{\arg\max}\left(\frac{\kappa_{K,j}}{w_{K,j}}\right)$$

and, then, we construct a minimal set $\mathcal{A}$ satisfying constraint (32) by using the SER algorithm from [10].

3.4 The Refinement Algorithms

In this section, we present the fully automatic refinement algorithms for goal-oriented adaptivity. These algorithms are based on our approach to goal-oriented error estimation presented in Section 3.2 and the hp-adaptive refinement strategy proposed above. Since this approach to goal-oriented adaptivity seems to be new for the classical h-adaptive case as well, we provide also a refinement algorithm for this case.
For the h-adaptive case, the algorithm looks very much like the one presented in [10]. We have only added steps to solve the dual problem (6) and to compute the solutions of the local variational problems (8). The resulting fully automatic h-adaptive refinement algorithm is shown in Algorithm 1.
The refinement algorithm for the hp-adaptive case, now, looks very much the same as the one proposed

(S0) Initialize coarse grid $\mathcal{T}_0$, choose $\theta\in(0,1]$ and TOL >0, and set $N:=0$.

(S1) Solve primal problem (4).

(S2) Solve dual problem (6).

(S3) For every $K\in\mathcal{T}_N$: Solve local variational problem (8).

(S4) Compute a posteriori error estimator from Definition 4.

(S5) If $\zeta\leq$ TOL: STOP

(S6) Refine cells according to fixed fraction scheme (29).

(S7) Set $N:=N+1$ and goto step (S1).

Algorithm 1: The fully automatic h-adaptive refinement algorithm.

for h-adaptive refinement in Algorithm 1. We only add one step to compute the convergence indicators $\kappa_{K,j}$. The resulting fully automatic hp-adaptive refinement algorithm is shown in Algorithm 2.

(S0) Initialize coarse grid $\mathcal{T}_0$, choose $\theta \in (0,1]$ and TOL > 0, and set $N := 0$.

(S1) Solve primal problem (4).

(S2) Solve dual problem (6).

(S3) For every $K \in \mathcal{T}_N$ solve local variational problem (8).

(S4) Compute a posteriori error estimator from Definition 4.

(S5) If $\zeta \leq$ TOL: STOP

(S6) For every $K \in \mathcal{T}_N$ and every $j \in \{1, \ldots, n\}$: Compute convergence indicator $\kappa_{K,j}$ as proposed in Section 3.3.2.

(S7) Refine cells according to the modified fixed fraction scheme (32).

(S8) Set $N := N + 1$ and goto step (S1).

Algorithm 2: The fully automatic *hp*-adaptive refinement algorithm.

4 Convergence

In this section, we want to prove convergence of the fully automatic goal-oriented adaptive refinement algorithms presented in Section 3.4. First, we will consider the case of *h*-adaptive refinement and, afterwards, the case of *hp*-adaptive refinement.
Before we prove the actual convergence results, let us state an auxiliary result which will be useful in the proofs later on.

Lemma 7. *Let $u \in H_0^1(\Omega)$ be the solution of (3) and $u_{FE} \in V^p(\mathcal{T})$ be the solution of (4). Further, let $z \in H_0^1(\Omega)$ be the solution of (5) and $z_0 \in V^p(\mathcal{T}_0)$ be the solution of (6) on some coarse grid $\mathcal{T}_0 \subseteq \mathcal{T}$. Then, it holds*

$$|J(u) - J(u_{FE})| \leq \|\nabla (z - z_0)\|_{L^2(\Omega)} \|\nabla (u - u_{FE})\|_{L^2(\Omega)}.$$

Proof. From dual problem (5), it follows

$$J(u) = \int_\Omega (\nabla z)^T \nabla u$$

and

$$J(u_{\mathrm{FE}}) = \int_\Omega (\nabla z)^T \nabla u_{\mathrm{FE}}.$$

Then, it follows

$$\begin{aligned} J(u) - J(u_{\mathrm{FE}}) &= \int_\Omega (\nabla z)^T \nabla (u - u_{\mathrm{FE}}) \\ &= \int_\Omega (\nabla (z - z_0))^T \nabla (u - u_{\mathrm{FE}}) \end{aligned}$$

with the Galerkin orthogonality

$$\int_\Omega (\nabla z_0)^T \nabla (u - u_{\mathrm{FE}}) = 0$$

and the result follows with the Cauchy-Schwarz inequality. □

4.1 h-Adaptive Refinement

Let us consider the case of h-adaptive refinement first. Here, the following convergence result holds.

Theorem 6 (Convergence (h-adaptive)). *Let $N \in \mathbb{N}$ and $r \in \mathbb{N}_0$ be arbitrary and $u \in H_0^1(\Omega)$ be the solution of (3). Further, let $\mathcal{A}_N \subseteq \mathcal{T}_N$ be such that (29) holds for some $\theta \in (0,1]$. Let $u_N \in V^p(\mathcal{T}_N)$, where $p = (r)_{K\in\mathcal{T}_N}$, be the solution of (4) in iteration step N and $z_0 \in V^p(\mathcal{T}_0)$, where $p = (r)_{K\in\mathcal{T}_0}$, be the solution of (6) on coarse grid $\mathcal{T}_0$. Additionally, let us assume that there exists some $\tau \in (0,1)$ sufficiently small such that*

$$\sum_{K\in\mathcal{T}_n} h_K^2 \|f - \Pi f\|_{L^2(K)}^2 \leq \tau^2 \eta\left(u_n, \Pi f\right)^2$$

for all $n \in \{0, \ldots, N-1\}$. Then, there exists some $\nu \in (0,1)$ independent of mesh size vector h such that

$$|J(u) - J(u_{FE})| \leq \nu^N \|\nabla(z - z_0)\|_{L^2(\Omega)} \|\nabla(u - u_0)\|_{L^2(\Omega)}.$$

Proof. Let $K \in \mathcal{A}_N$ be arbitrary. Since $\mathcal{A}_N$ has minimal cardinality, it holds

$$0 < \zeta_K = \rho_K \eta_K\left(u_N, \Pi f\right)$$

and, thus, $\eta_K(u_N, \Pi f) > 0$. Then, we have

$$\sum_{K\in\mathcal{A}_N} \eta_K\left(u_N, \Pi f\right)^2 \geq \theta_N^2 \eta\left(u_N, \Pi f\right)^2$$

for

$$\theta_N^2 := \frac{1}{\eta\left(u_N, \Pi f\right)^2} \sum_{K\in\mathcal{A}_N} \eta_K\left(u_N, \Pi f\right)^2 \in (0,1]$$

and Theorem 4 yields

$$\|\nabla(u - u_N)\|_{L^2(\Omega)} \leq \nu(\theta_N) \|\nabla(u - u_{N-1})\|_{L^2(\Omega)}. \tag{33}$$

From Lemma 7, we have

$$\begin{aligned} |J(u) - J(u_N)| &\leq \|\nabla(z - z_0)\|_{L^2(\Omega)} \|\nabla(u - u_N)\|_{L^2(\Omega)} \\ &\leq \prod_{i=1}^{N} \nu(\theta_i) \|\nabla(z - z_0)\|_{L^2(\Omega)} \|\nabla(u - u_0)\|_{L^2(\Omega)} \end{aligned}$$

by applying estimate (33) iteratively and the result follows. □

4.2 hp-Adaptive Refinement

For hp-adaptive refinement, convergence can be shown quite similarly to the case of h-adaptive refinement.

Theorem 7 (Convergence (hp-adaptive)). *Let $N \in \mathbb{N}$ be arbitrary and $u \in H_0^1(\Omega)$ be the solution of (3). Further, let $\left(\mathcal{A}_N, (j_K)_{K\in\mathcal{A}_N}\right)$ be a solution of (30), (32) for some $\theta \in (0,1]$. Let $u_N \in V^p(\mathcal{T}_N)$ be the solution of (4) in iteration step N and $z_0 \in V^p(\mathcal{T}_0)$ be the solution of (6) on coarse grid $\mathcal{T}_0$. Additionally, let us assume that there exists some $\tau \in (0,1)$ sufficiently small such that*

$$\sum_{K\in\mathcal{T}_n} \frac{h_K^2}{p_K^2} \|f - \Pi f\|_{L^2(K)}^2 \leq \tau^2 \eta\left(u_n, \Pi f\right)^2$$

for all $n \in \{0, \ldots, N-1\}$. Then, there exists some $\nu \in (0,1)$ independent of mesh size vector h and polynomial degree vector p such that

$$|J(u) - J(u_{FE})| \leq \nu^N \|\nabla(z - z_0)\|_{L^2(\Omega)} \|\nabla(u - u_0)\|_{L^2(\Omega)}.$$

Proof. Let $K \in \mathcal{A}_N$ be arbitrary. Since $\mathcal{A}_N$ has minimal cardinality, it holds

$$0 < \kappa_{K,j_K}\zeta_K = \kappa_{K,j_K}\rho_K\eta_K\left(u_N, \Pi f\right)$$

and, thus, $\kappa_{K,j_K}\eta_K\left(u_N, \Pi f\right) > 0$. Then, we have

$$\sum_{K \in \mathcal{A}_N} \kappa^2_{K,j_K}\eta_K\left(u_N, \Pi f\right)^2 \geq \theta_N^2 \eta\left(u_N, \Pi f\right)^2$$

for

$$\theta_N^2 := \frac{1}{\eta\left(u_N, \Pi f\right)^2} \sum_{K \in \mathcal{A}_N} \kappa^2_{K,j_K}\eta_K\left(u_N, \Pi f\right)^2 \in (0, 1]$$

and Theorem 5 yields

$$\left\|\nabla\left(u - u_N\right)\right\|_{L^2(\Omega)} \leq \nu\left(\theta_N\right)\left\|\nabla\left(u - u_{N-1}\right)\right\|_{L^2(\Omega)}. \tag{34}$$

From Lemma 7, we have

$$\begin{aligned}\left|J(u) - J\left(u_N\right)\right| &\leq \left\|\nabla\left(z - z_0\right)\right\|_{L^2(\Omega)}\left\|\nabla\left(u - u_N\right)\right\|_{L^2(\Omega)} \\ &\leq \prod_{i=1}^{N} \nu\left(\theta_i\right)\left\|\nabla\left(z - z_0\right)\right\|_{L^2(\Omega)}\left\|\nabla\left(u - u_0\right)\right\|_{L^2(\Omega)}\end{aligned}$$

by applying estimate (34) iteratively and the result follows. □

5 Numerical Results

In this section we perform numerical illustrations to show the performance of the presented method. From now on, we use the following acronyms: BN is our algorithm presented in this paper; MS stands for algorithm presented in Mommer and Stevenson [22]; HP is the one proposed by Holst and Pollock [16]; Jo the dual weighted error estimates used in Johnson et.al. [18, 12]; and finally En is residual based error estimation of the energy norm as in Definition 2, see e.g. [10, 8]. We have already mentioned the difference between MS and HP earlier, but let us recall it here for completeness.

Let $\mathcal{M}_p$ be the set of cells with the largest energy indicator $\eta_K\left(u_{\mathrm{FE}}, \Pi f\right)$, $K \in \mathcal{T}$ of the primal problem defined in Definition 2, such that

$$\sum_{K \in \mathcal{M}_p} \eta_K\left(u_{\mathrm{FE}}, \Pi f\right)^2 \geq \theta^2 \eta\left(u_{\mathrm{FE}}, \Pi f\right)^2.$$

Similarly, let $\mathcal{M}_d$ be the set of cells with the largest energy indicator $\eta_K\left(z_{\mathrm{FE}}, \Pi j\right)$, $K \in \mathcal{T}$ of the dual problem, such that

$$\sum_{K \in \mathcal{M}_d} \eta_K\left(z_{\mathrm{FE}}, \Pi j\right)^2 \geq \theta^2 \eta\left(z_{\mathrm{FE}}, \Pi j\right)^2.$$

For the refinement MS chooses the set with the smallest cardinality between $\mathcal{M}_p$ and $\mathcal{M}_d$, whereas HP uses the union of these sets $\mathcal{M}_p \cup \mathcal{M}_d$.

For the dual-weighted residual the error on the target functional is written in the form of

$$J(u) - J(u_{FE}) = \int_\Omega (-\Delta u_{\mathrm{FE}} - \Pi f) z,$$

and the Galerkin orthogonality results to

$$J(u) - J(u_{FE}) = \int_{\Omega} (-\Delta u_{\rm FE} - \Pi f)(z - \pi z),$$

where πz is an interpolation of the dual solution into the primal finite element space. The last formulation is usually used by Becker, Rannacher, Giles, Süli, Hartmann, Houston, etc, see e.g. [4, 13, 14]. The advantage of the last estimator is that it can be easily divided between the cells, moreover the estimator is sharp. However, the space of the dual solution should be at least one order higher than the one that the primal solution lives. Johnson and coworkers [18, 12] suggest to use the standard interpolation estimate on the last relation and obtain

$$|J(u) - J(u_{FE})| \leq C \sum_{K \in \mathcal{T}} h^{\alpha} \| - \Delta u_{\rm FE} - \Pi f\|_{L^2(K)} \|D^{\alpha} z\|_{L^2(K)},$$

where C is a constant of the interpolation estimates, $\alpha = 1$ or 2. Further they define a stability factor $S = \|D^{\alpha} z\|_{L^2(\Omega)}$, which measures certain stability properties of the dual problem with respect to the target functional. Due to the interpolation estimate the error in the target functional is overestimated. However, the main advantage of this error estimate is that the dual solution can live at the same finite element space as the primal solution, which can be cheaper to compute computationally. In our numerical computations we use $\alpha = 1$ and $C = \frac{1}{2}$.
The implementation is done with two open source finite element libraries: DOLFIN and deal.II, see [19, 1]. Implementation of h-adaptivity in triangular meshes is done in DOLFIN in the framework of Unicorn solver [15]. Then fully automatic hp-adaptivity is implemented in deal.ii for quadrilateral elements. The Döfler marking coefficient is chosen $\theta = 0.5$ for all computations shown below.

5.1 L-shaped domain

Consider the Poisson equation is solved in a L-shaped domain $\Omega = (-1, 1)^2 \backslash [0, 1) \times (-1, 0]$ with the right hand side function $f = 0$. The boundary condition is set such that the exact solution to this problem is $u(r, \phi) = r^{\frac{2}{3}} \sin(\frac{2}{3}\phi)$. The solution has singularity at corner $(0, 0)$. We are interested on the point error at $(x, y) = (\frac{\pi}{6}, \frac{\pi}{6})$. Therefore we set the right hand side of the dual problem as a delta function at the given point $j(x, y) = \exp(-10^4((x - \frac{\pi}{6})^2 + (y - \frac{\pi}{6})^2))$.
The result of the computations is collected in Figure 2. In all plots the dashed line is $N^{-1} := (C_N \cdot \#nodes)^{-1}$, where C_N is chosen such that the dashed line lies always on the top of all other lines. The left plot describes the true functional error from all computations. We can see that the errors decrease linearly with respect to number of nodes of the mesh. The middle plot is estimated errors for each adaptive iterations. One can see that the energy error is the worse with respect to the rate and value. HP has the optimal rate but as expected it has a bigger value than MS for example. There is no convergence or optimality known for Jo is known, even though the estimator is sharp for coarse meshes the rate does not seem to be optimal. BN performs as good as MS for this test case.
The meshes with almost the same number of nodes after some adaptive iterations are shown in Figure 3. Since the primal solution has singularly at corner $(0, 0)$ the energy estimator marks only the neighborhood close to the singularity. MS and HP behave almost the same as expected; both cells with the highest primal and dual residuals are refined. Jo multiplies a weight to the primal residual, therefore area with respect to the error of the functional or larger dual solution is refined. The same behavior can be observed for the BN refinement.
At last, one has to mention that in order to get the same amount of mesh points for the finest mesh BN needs 20, En needs 80, HP needs 25, MS needs 50 and Jo needs 20 adaptive iterations. We see that even though MS is optimal it takes twice more iterations for the same error obtained by BN.

We solved the same problem using quadrilateral elements in deal.ii. Here we use fully *hp*-adaptive algorithm that we presented earlier in this paper using the method BN. The computational results are presented in Figure 4, where the change in the polynomial degree and the mesh is plotted. One can see that the polynomials of higher degrees are used in the smooth region, while the mesh is instead refined in the region with sharp discontinuity. The exponential decay of error can be observed from the figure on the right panel.

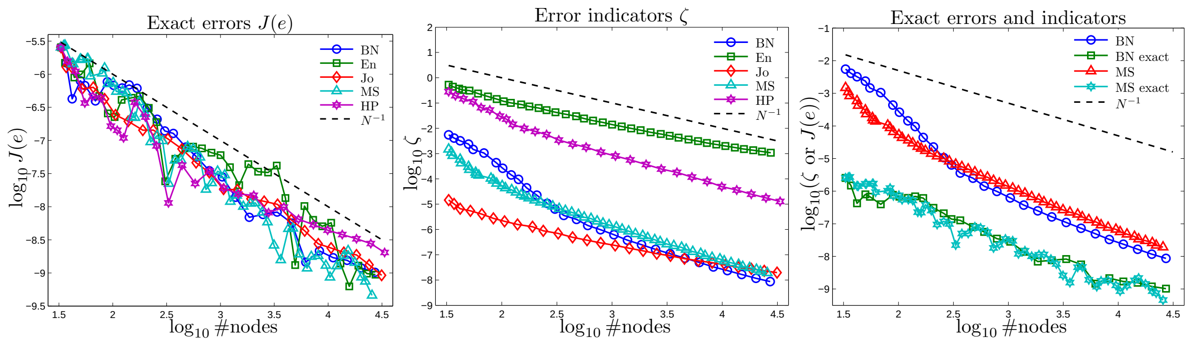

Figure 2: L-shaped domain: Exact functional error (left), Error indicators (center), comparison of MS and BN (right)

5.2 Square-annulus

Consider the Poisson equation is solved in a square-annulus, where the domain is $\Omega = [-1,1]\times[-1,1]\backslash[-\frac{2}{6},\frac{2}{6}]\times[-\frac{2}{6},\frac{2}{6}]$. The right hand side of the primal problem $f(x,y)$ is chosen such that the exact solution is

$$u(x,y) = \frac{\sin(\pi\omega x)\sin(\pi\omega y)}{(x-0.2)^2+(y-0.2)^2+10^{-10}}.$$

The initial mesh consists of 500 cells and 288 $\mathbb{P}1$ nodes. We are interested in two target functionals: (a) $J(u) = \int_{\Omega_1} u$, where $\Omega_1 = [-0.8,-0.4]\times[-0.8,-0.4]$; and (b) $J(u) = \int_{\Omega_2} u$, where $\Omega_2 = [-0.8,-0.4]\times[0.4,0.8]$. In the computation of the dual problem the source term is set to be 1 inside Ω_1 or Ω_2 and 0 otherwise. The primal and dual solutions are shown in Figure 5.

We report the result of the adaptive iterations from different methods in Figure 6 for case (a) and Figure 8 for case (b). Again C_N is chosen such that N^{-1} lies always on the top of all other lines. We observe the best true error is obtained by BN for case (a) and Jo for case (b). The results of the error indicators show that MS, HP and BN have the same convergence rate for both cases. Moreover, BN has a sharper estimator for finer meshes. Also for these test cases, MN took twice more adaptive iterations than BN for the same accuracy.

The meshes with almost the same number of nodes are presented in Figures 7 and 9. The primal residual is high close to the interior upper right corner and the dual residual is high close to Ω_1 and Ω_2. En focuses the cells where the primal residual is high, therefore the refinement is done on the upper right side of the domain. MS and HP behave similarly, the refinement is done for both cells with the largest primal and dual residuals. However, Jo and BN do not refine the cells with the largest primal residual, it is more clear in case (a).

In conclusion, we see that BN behaves the same as original dual-weighted residual method proposed in the literature. Also the performance is as good as MS and HP with respect to the error and optimality.

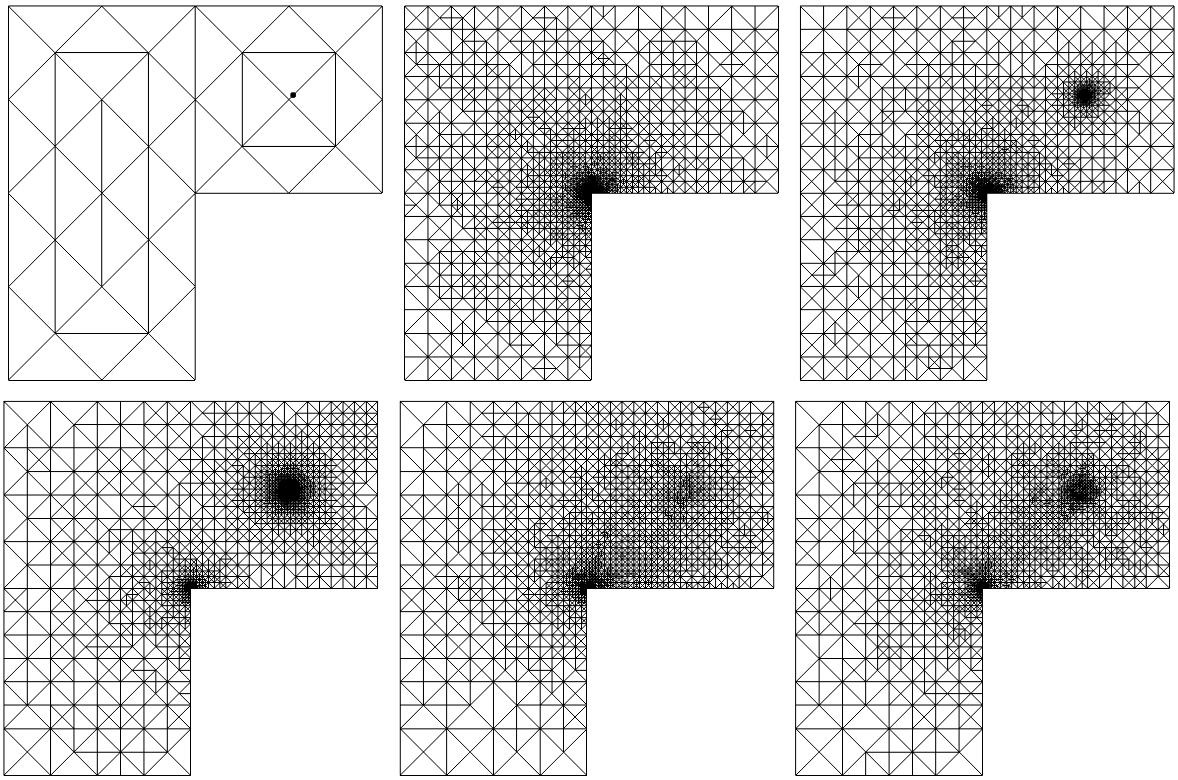

Figure 3: L-shaped domain: the target functional is the error at point $(x, y) = (\frac{\pi}{6}, \frac{\pi}{6})$. First row: the initial mesh with 33 $\mathbb{P}1$ nodes and 48 triangles (left); En 1813 $\mathbb{P}1$ nodes (middle); MS 1898 $\mathbb{P}1$ nodes (right). Second row: HP 2038 $\mathbb{P}1$ nodes (left); Jo 1916 $\mathbb{P}1$ nodes (middle); BN 1851 $\mathbb{P}1$ nodes (right).

Remark 1. *Note that in step (S3) of Algorithms 1 and 2 the patch problems, which are additional boundary value problems, are solved for each element. In fact construction of submeshes and solving the PDE on them are very time-consuming. Figure 10 plots the total estimated error vs total computational time for each full circle of adaptive algorithms for different methods for triangular meshes. We denote by "BN X layer" the result of Algorithm 1 with X layer, i.e. the patch is $\omega_{K,X}$ in (1). It is obvious that MS algorithm is faster than BN to produce the same error, however BN needs 10 iterations while MS needs 25 iterations to produce the smallest error in this test. The usual goal oriented algorithm such as Jo becomes more expensive than BN after a certain given tolerance. Given the fact that the BN algorithm behaves similarly for different layers, it is feasible to use smaller layers in the applications.*

6 Conclusion

In this paper a new approach for goal-oriented adaptive finite element methods is presented. The novelty consists of applying Clément and Scott-Zhang type interpolation operators to get the dual-weighted error estimate locally for each cell. This approach allows us to enjoy cell based error estimates as well as the proof of reliability, efficiency and convergence. To the best of our knowledge, these interpolation operators are successfully used for energy based h and hp adaptive algorithm in the past, however this paper is the first result for the goal-oriented finite elements in this direction. The numerical illustrations confirm

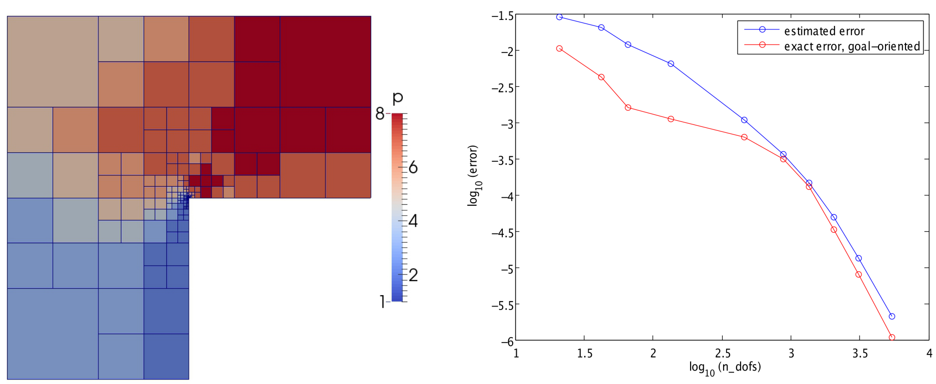

Figure 4: L-shaped domain: The target functional is the error at point $(x, y) = (\frac{\pi}{6}, \frac{\pi}{6})$. Left: Distribution of polynomial degree and local elements. Right: Convergence of the estimated error together with the exact error.

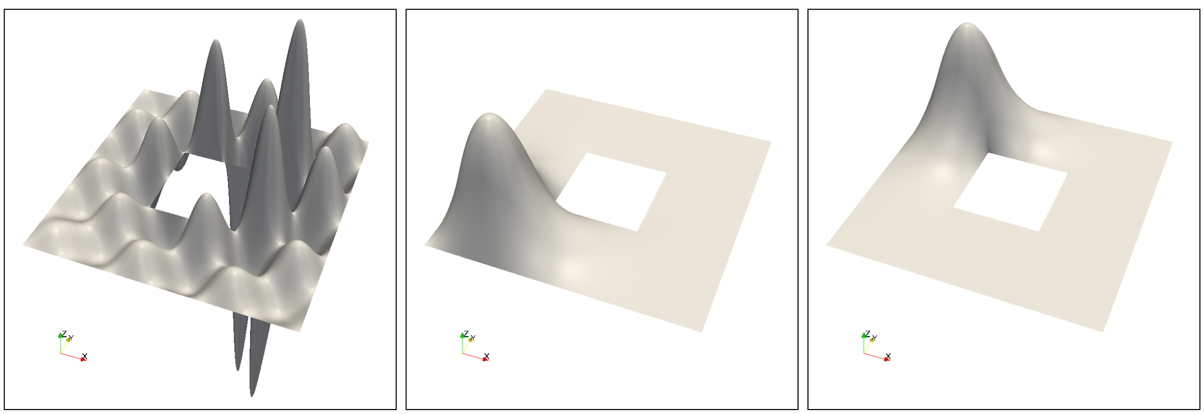

Figure 5: Square-annulus. The primal solution (left), dual solution for case (a) (center), dual solution for case (b) (right)

the presented theory and compared with several existing algorithms. The method can be extended for other PDE's which is one of our the main current research. The optimality of the algorithm is tested numerically, however we are investigating to prove it a priori. The results of application of the method to other PDE's and optimality results will be reported in due time.

References

[1] W. Bangerth, R. Hartmann, and G. Kanschat. deal.II – a general purpose object oriented finite element library. *ACM Trans. Math. Softw.*, 33(4):24/1–24/27, 2007.

[2] R. Becker and R. Rannacher. A feed-back approach to error control in finite element methods: basic analysis and examples. *East-West J. Numer. Math.*, 4:237–264, 1996.

[3] R. Becker and R. Rannacher. Weighted a posteriori error control in FE methods. In H.G. Bock et. al., editor, *Proc. ENUMATH-97*, pages 621–637, Singapore, 1997. World Scientific Publ.

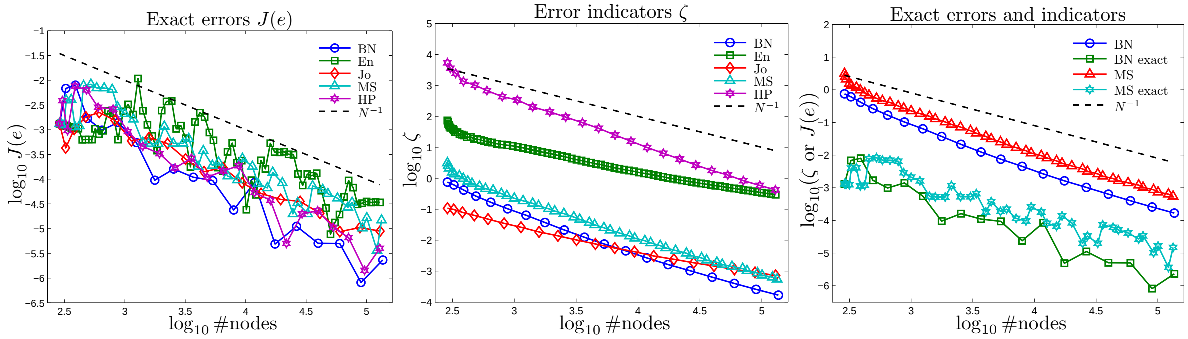

Figure 6: Square-annulus. The target function is the average value of the solution at Ω_1. Exact functional error (left), Error indicators (center), comparison of MS and BN (right)

[4] Roland Becker and Rolf Rannacher. A feed-back approach to error control in adaptive finite element methods: Basic analysis and examples. *East-West J. Numer. Math.*, 4:237–264, 1996.

[5] M. Bürg. *A Fully Automatic hp-Adaptive Refinement Strategy*. PhD thesis, Research Training Group 1294, Karlsruhe Institute of Technology (KIT), July 2012.

[6] M. Bürg. Convergence of an Automatic *hp*-Adaptive Finite Element Strategy for Maxwell's Equations. *Appl. Numer. Math.*, 72:188–206, 2013.

[7] M. Bürg and W. Dörfler. Convergence of an adaptive *hp* finite element strategy in higher space-dimensions. *Appl. Numer. Math.*, 61:1132–1146, 2011.

[8] J. Cascon, C. Kreuzer, R. Nochetto, and K. Siebert. Quasi-optimal convergence rate for an adaptive finite element method. *SIAM Journal on Numerical Analysis*, 46(5):2524–2550, 2008.

[9] Th.H. Cormen, C.E. Leiserson, R. Rivest, and C. Stein. *Introduction to Algorithms*. MIT Press, Cambridge, MA, 2001.

[10] W. Dörfler. A convergent adaptive algorithm for Poisson's equation. *SIAM J. Numer. Anal.*, 33(3):1106–1124, 1996.

[11] W. Dörfler and V. Heuveline. Convergence of an adaptive *hp* finite element strategy in one space dimension. *Appl. Numer. Math.*, 57:1108–1124, 2007.

[12] Kenneth Eriksson, Don Estep, Peter Hansbo, and Claes Johnson. Introduction to adaptive methods for differential equations. *Acta Numer.*, 4:105–158, 1995.

[13] M. Giles and E. Süli. Adjoint methods for pdes: a posteriori error analysis and postprocessing by duality. *Acta Numer.*, 11:145–236, 2002.

[14] Ralf Hartmann and Paul Houston. Adaptive discontinuous Galerkin finite element methods for nonlinear hyperbolic conservation laws. *SIAM J. Sci. Comp.*, 24:979–1004, 2002.

[15] Johan Hoffman, Johan Jansson, Cem Degirmenci, Niclas Jansson, and Murtazo Nazarov. Unicorn: a unified continuum mechanics solver. In Anders Logg, Kent-Andre Mardal, and Garth Wells, editors, *Automated Solution of Differential Equations by the Finite Element Method*, volume 84 of *Lecture Notes in Computational Science and Engineering*, pages 339–361. Springer Berlin Heidelberg, 2012.

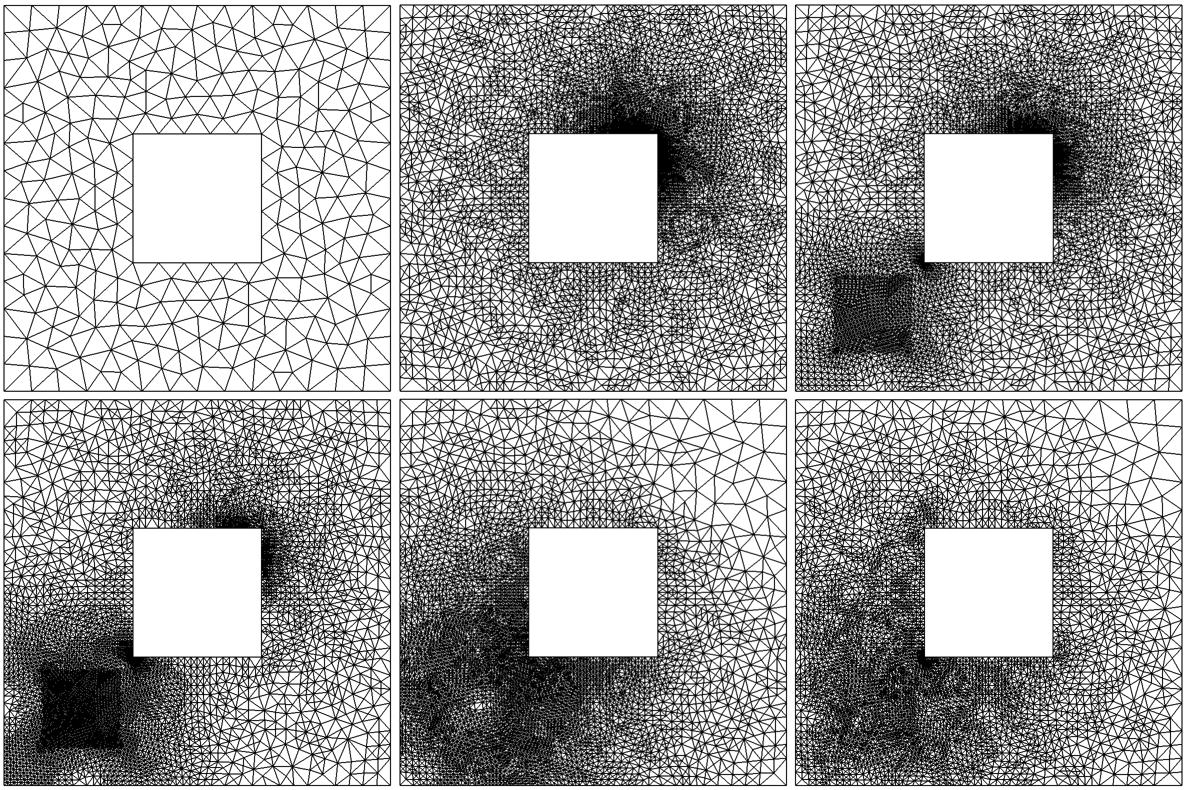

Figure 7: Square-annulus. Case (a). First row: the initial mesh with 288 $\mathbb{P}1$ nodes and 500 triangles (left); En 5914 $\mathbb{P}1$ nodes (middle); MS 5947 $\mathbb{P}1$ nodes (right). Second row: HP 6522 $\mathbb{P}1$ nodes (left); Jo 6488 $\mathbb{P}1$ nodes (middle); BN 5337 $\mathbb{P}1$ nodes (right).

[16] Michael Holst and Sara Pollock. Convergence of goal-oriented adaptive finite element methods for nonsymmetric problems, 2011.

[17] Niclas Jansson, Johan Hoffman, and Murtazo Nazarov. Adaptive simulation of turbulent flow past a full car model. In *State of the Practice Reports*, SC '11, pages 20:1–20:8, New York, NY, USA, 2011. ACM.

[18] C. Johnson and A. Szepessy. Adaptive finite element methods for conservation laws based on a posteriori error estimates. *Commun. Pure. Appl. Math*, 48:199–234, 1995.

[19] Anders Logg and Garth N. Wells. DOLFIN: automated finite element computing. *ACM Trans. Math. Software*, 37(2):Art. 20, 28, 2010.

[20] J.M. Melenk. *hp*-Interpolation of nonsmooth functions and an application to *hp*-a posteriori error estimation. *SIAM J. Numer. Anal.*, 43(1):127–155, 2005.

[21] J.M. Melenk and B.I. Wohlmuth. On residual-based a posteriori error estimation in *hp*-FEM. *Adv. Comp. Math.*, 15:311–331, 2001.

[22] M.S. Mommer and R. Stevenson. A Goal-Oriented Adaptive Finite Element Method with Convergence Rates. *SIAM J. Numer. Anal.*, 47(2):861–886, 2009.

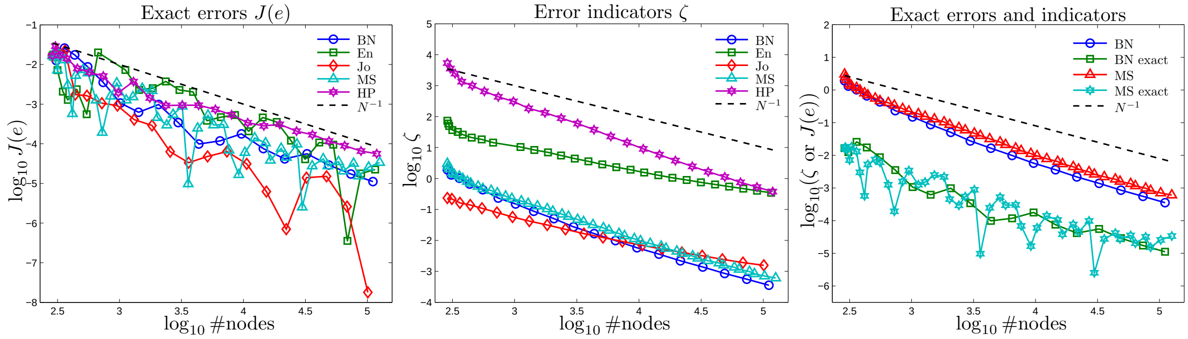

Figure 8: Square-annulus. The target function is the average value of the solution in Ω_2. Exact functional error (left), Error indicators (center), comparison of MS and BN (right)

[23] K.-S. Moon, E. von Schwerin, A. Szepessy, and R. Tempone. Convergence rates for an adaptive dual weighted residual finite element algorithm. *BIT Numerical Mathematics*, 46(2):367–407, 2006.

[24] Murtazo Nazarov and Johan Hoffman. An adaptive finite element method for inviscid compressible flow. *International Journal for Numerical Methods in Fluids*, 64(10-12):1102–1128, 2010.

[25] Murtazo Nazarov and Johan Hoffman. Residual-based artificial viscosity for simulation of turbulent compressible flow using adaptive finite element methods. *International Journal for Numerical Methods in Fluids*, 71(3):339–357, 2013.

[26] J. T. Oden and S. Prudhomme. On goal-oriented error estimation for elliptic problems: Application to the control of pointwise errors. *Comput. Meth. Appl. Mech. Eng.*, 111:185–202, 1999.

[27] R. Rannacher. Error control in finite element computations. In H. Bulgak and C. Zenger, editors, *Error Control and Adaptivity in Scientific Computing*, NATO Science Series, pages 247–278, Dortrech, 1999. Proc. NATO-Summer School, Kluwer Academic Publ.

[28] M-C. Rivara. Local modification of meshes for adaptive and/or multigrid finite-element methods. *Journal of Computational and Applied Mathematics*, 36(1):78–89, 1992.

[29] Ch. Schwab. *p- and hp-Finite Element Methods*. Clarendon Press, Oxford, 1998.

[30] L.R. Scott and S. Zhang. Finite element interpolation of nonsmooth functions satisfying boundary conditions. *Math. Comp.*, 54:483–493, 1990.

[31] B. Szabó and I. Babuška. *Finite Element Analysis*. Wiley, New York, NY, 1991.

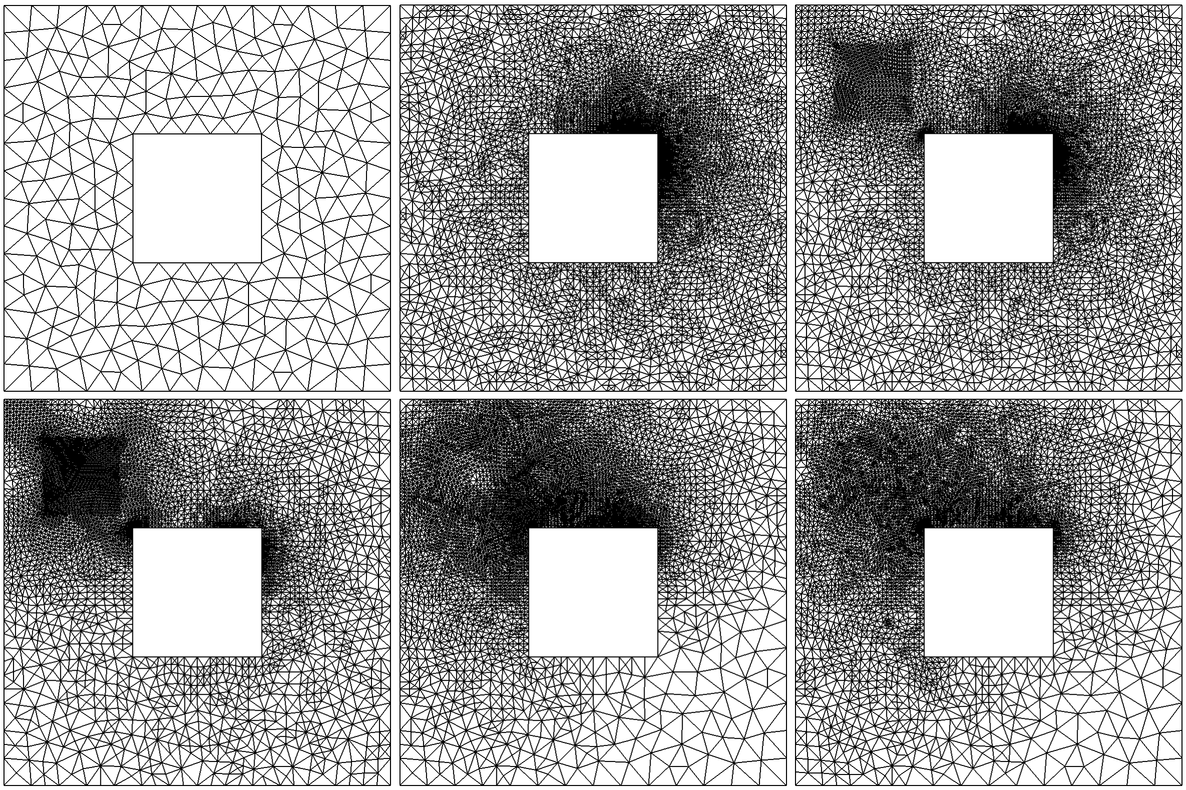

Figure 9: Square-annulus. Case (b). First row: the initial mesh with 288 $\mathbb{P}1$ nodes and 500 triangles (left); En 6578 $\mathbb{P}1$ nodes (middle); MS 6913 $\mathbb{P}1$ nodes (right). Second row: HP 5932 $\mathbb{P}1$ nodes (left); Jo 7355 $\mathbb{P}1$ nodes (middle); BN 6474 $\mathbb{P}1$ nodes (right).

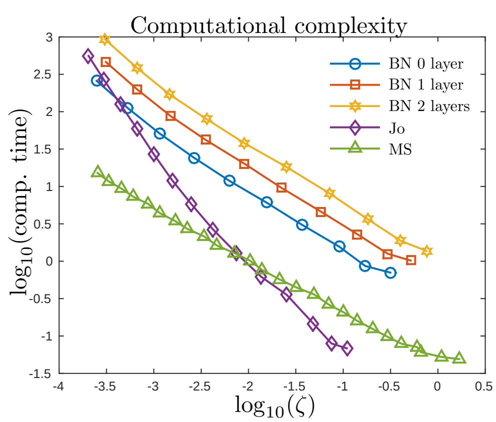

Figure 10: Square-annulus. Case (b). Computational complexity of different algorithms.